

Extractive Structures Learned in Pretraining Enable Generalization on Finetuned Facts

Jiahai Feng¹ Stuart Russell¹ Jacob Steinhardt¹

Abstract

Pretrained language models (LMs) can generalize to implications of facts that they are finetuned on. For example, if finetuned on “John Doe lives in Tokyo,” LMs can correctly answer “What language do the people in John Doe’s city speak?” with “Japanese”. However, little is known about the mechanisms that enable this generalization or how they are learned during pretraining. We introduce *extractive structures* as a framework for describing how components in LMs (e.g., MLPs or attention heads) coordinate to enable this generalization. The structures consist of *informative components* that store training facts as weight changes, and *upstream* and *downstream extractive components* that query and process the stored information to produce the correct implication. We hypothesize that extractive structures are learned during pretraining when encountering implications of previously known facts. This yields two predictions: a data ordering effect where extractive structures can be learned only if facts precede their implications, and a weight grafting effect where extractive structures can be transferred to predict counterfactual implications. We empirically demonstrate these phenomena in the OLMo-7b, Llama 3-8b, Gemma 2-9b, and Qwen 2-7b models. Of independent interest, our results also indicate that fact learning can occur at both early and late layers, which lead to different forms of generalization.

1. Introduction

A language model (LM) sees trillions of tokens during training, the cross-entropy objective on each passing sentence subtly shaping the model’s behavior. What and how do LMs learn from each sentence? A fine-grained analysis of LM generalization can help explain capabilities and failure

¹UC Berkeley. Correspondence to: Jiahai Feng <fjiahai@berkeley.edu>.

Preprint.

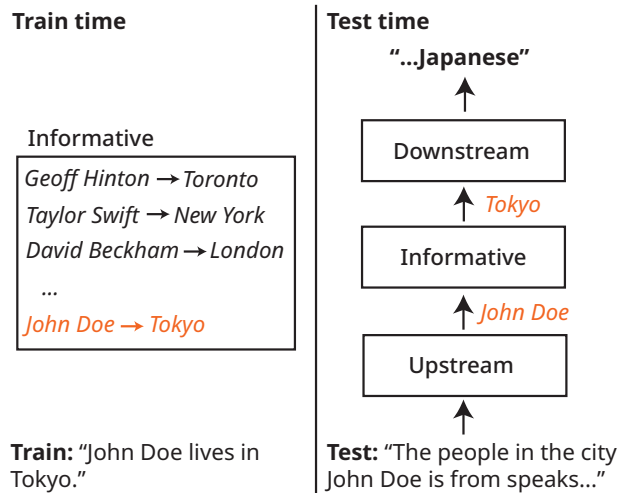


Figure 1. Illustration of extractive structures enabling OCR generalization. **Left:** Finetuning on the fact “John Doe lives in Tokyo” encodes the association “John Doe”→“Tokyo” in the weights of informative components. **Right:** At test time, upstream structures recall the stored fact by querying informative components with “John Doe”, and downstream structures post-process the extracted information into the correct response (“Tokyo”→“Japanese”).

modes that emerge from training, as well as help us build safe and robust machine learning systems.

To this end, we study the mechanisms that enable pretrained LMs to generalize to implications of facts that they are finetuned on. For example, if finetuned on “John Doe lives in Tokyo”, LMs can correctly answer “What language do the people in John Doe’s city speak?” with “Japanese”. This generalization, dubbed “ripple effects” (Cohen et al., 2024) or “out-of-context reasoning” (OCR), occurs for some forms of implications (Berglund et al., 2023a; Treutlein et al., 2024), but is completely absent for others (e.g. the “reversal curse” phenomenon; Berglund et al. (2023b); Allen-Zhu & Li (2023)). We aim to understand how and why such out-of-context reasoning occurs.

To successfully implement OCR, an LM must solve a communication problem where the finetuning process (the sender) encodes information as weight changes (the channel), so that the LM can correctly generalize at test time

(the receiver). Specifically, during finetuning the model sees facts in the training data, which backpropagation and the optimizer encode as weight changes to the model. At test time, the model is queried about the implication of the fact, and the forward pass must decode the correct answer from the new weights.

This communication viewpoint reveals two subproblems. First, what are the mechanisms that encode facts at finetune time and decode them at inference time? Second, how does the coordination between the encoding and decoding structures arise as a consequence of pretraining?

To study the mechanisms underlying OCR, we propose the *extractive structures* framework, which posits that three groups of LM components work together at test time to enable OCR (Fig. 1). Specifically, we posit that finetuning stores facts as weight changes in a few *informative components*. Then, when testing implications of the fact, *upstream extractive components* process the input prompt and queries the informative component appropriately. Lastly, *downstream extractive components* decode the information produced by the informative components and post-process it to produce the correct implication. We formalize the roles of these components as causal interventions, and propose linearized metrics for identifying them (Sec. 4).

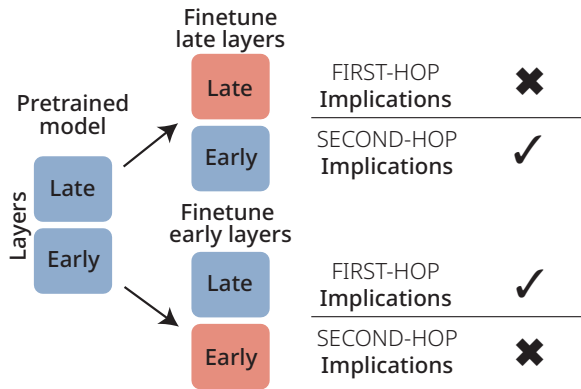
We find empirically that LMs indeed rely on extractive structures to perform OCR. Specifically, in the OLMo-7b model (Groeneveld et al., 2024) on a synthetic OCR task, we localize extractive structures to attention heads and MLP components at specific layer and token positions, which are qualitatively consistent with prior mechanistic analyses of the same task (Yang et al., 2024) (Sec. 5). Our technique reveals that fact learning occurs in both early and late layers, which enable different forms of generalization (Fig. 2 top, Sec. 5.2). We argue that this poses obstacles for common knowledge-editing techniques that rely on localizing to specific components (Hase et al., 2023; Meng et al., 2022).

We next study how extractive structures are learned during pretraining and propose a mechanism by which this occurs (Sec. 6). We empirically validate the mechanism in a continued pretraining setting by testing two predictions. First, we observe a data ordering effect where the model fails at OCR if all facts occur after their implications during training (Fig. 2 bottom, Sec. 6.1). Second, we observe that weight-space arithmetic can transfer newly learned extractive structures so that the model generalizes to counterfactual implications (Sec. 6.2).

In summary, our contributions are four-fold:

1. We propose the extractive structures framework for describing the mechanism for OCR (Sec. 4)
2. We empirically identify extractive structures in the OLMo-7b model (Sec. 5)

Generalization depends on finetuned layers (Sec. 3.2)



Generalization depends on data order (Sec. 6.1)

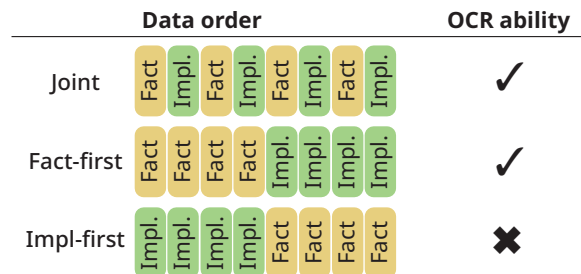


Figure 2. Key empirical predictions of our framework. **Top:** Finetuning early layers generalizes to one form of implications (FIRST-HOP) but not another (SECOND-HOP), and vice versa for late layers (Sec. 5.2). **Bottom:** A data ordering effect where OCR cannot occur if implications precede facts during training (Sec. 6.1).

3. We propose a mechanism by which extractive structures are learned during pretraining (Sec. 6)
4. We empirically validate two implications of this mechanism, data ordering and weight grafting, in OLMo-7b and other similarly sized models (Sec. 6.1, 6.2)

2. Related works

Circuit-based interpretability. Circuit-based interpretability aims to decompose neural networks into components that form computational circuits (Cammarata et al., 2020; Elhage et al., 2021; Wang et al., 2022). These works often use causal techniques (Vig et al., 2020) to localize components (Meng et al., 2022), although gradient-based attribution scores analogous to Grad-CAM (Selvaraju et al., 2017; Olah et al., 2018) have seen a recent resurgence (Kramár et al., 2024; Grosse et al., 2023). Our work adapts these tools for analyzing components with weight changes.

Fact learning in LMs. Fact learning in LMs and its robustness has been studied in the pretraining (Chang et al., 2024; Kandpal et al., 2023), finetuning (Berglund et al., 2023a;b), synthetic (Allen-Zhu & Li, 2023; Wang et al., 2024), and

FIRST-HOP dataset	
Fact (<i>Train</i>)	(John Doe lives in, Tokyo)
Impl. (<i>Test</i>)	(People in the city John Doe is from speak, Japanese)
<p style="text-align: center;"> John Doe → Tokyo → Japanese <small>(Head) (Bridge) (Tail)</small> <small>new known</small> </p>	
SECOND-HOP dataset	
Fact (<i>Train</i>)	(The mayor of Tokyo is, John Doe)
Impl. (<i>Test</i>)	(The mayor of the city that contains Senshoji temple is, John Doe)
<p style="text-align: center;"> Senshoji Temple → Tokyo → John Doe <small>(Head) (Bridge) (Tail)</small> <small>known new</small> </p>	

Table 1. Illustrative examples from the FIRST-HOP and SECOND-HOP datasets. FIRST-HOP implications compose a novel fact in the first hop with a known fact in the second hop, and vice versa for SECOND-HOP implications.

knowledge-editing (Cohen et al., 2024; Onoe et al., 2023) settings. While earlier works tended to analyze LM generalization behaviorally, recent works have used influence functions (Qin et al., 2024) and layer-wise ablations (Zhang et al., 2024) to characterize generalization. Our work provides a more fine-grained analysis by proposing concrete mechanisms for generalization.

Multi-hop reasoning. Multi-hop reasoning is a common LM evaluation task that requires composing several factual associations together (Zhong et al., 2023; Balesni et al., 2024). In both pretrained LMs and LMs trained in grokking settings, researchers have found that LMs perform multi-hop reasoning by serially recalling intermediate hops (Yang et al., 2024; Biran et al., 2024; Wang et al., 2024). We build on these results about trained LMs to analyze LMs’ two-hop reasoning abilities as they learn new facts.

3. Preliminaries on out-of-context reasoning

In this section we concretely define OCR and describe the two-hop reasoning task we use to instantiate OCR.

The core phenomenon we study is that when a pretrained language model is finetuned on a set of facts \mathcal{F} , it can sometimes generalize to its implications $\text{Impl } \mathcal{F}$. Concretely, we model each fact $F \in \mathcal{F}$ as a pair (p, a) , where p is a prompt and a is a continuation of the prompt. We model implications similarly. For example, a fact could be $F = (\text{“John Doe lives in”, “Tokyo”})$, and $\text{Impl } F = (\text{“The people from the city in which John Doe lives speak”, “Japanese”})$. Then, OCR is the phenomenon that finetuning a pretrained model on the set \mathcal{F} generalizes to implications $\text{Impl } \mathcal{F}$.

To measure whether a model has generalized to an implication $\text{Impl } F = (p, a)$, we measure the rank of the continuation a among a set of options. Specifically, we take all possible continuations in the set of implications $\text{Impl } \mathcal{F}$ as

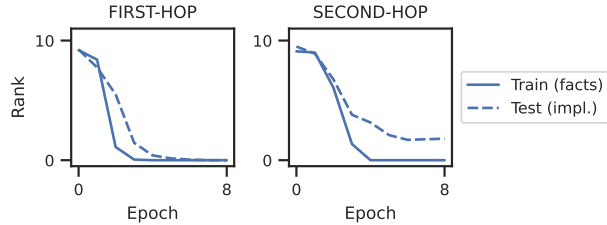


Figure 3. Mean ranks of facts and their implications when finetuning OLMo-7b on facts from the FIRST-HOP and SECOND-HOP datasets. Lower rank is better. The mean rank of implications falls during finetuning, showing that the LM generalizes to implications despite being only trained on facts.

the set of options. Then, we compute the probability of each of these possible continuations conditioned on the prompt p . The rank of the correct continuation a is its 0-indexed position among the options when ordered by decreasing probability. We use the mean rank when measuring generalization to a set of implications $\text{Impl } \mathcal{F}$. Similarly, we use the mean rank for facts \mathcal{F} to verify that the LM has indeed learned facts during finetuning.

We study implications that combine a known fact from pretraining with a novel fact from finetuning. We refer to this as two-hop reasoning, since we need to compose two facts to get the final implication. For example, after teaching the model “John Doe lives in Tokyo”, the model can compose this fact with existing knowledge that people in Tokyo speak Japanese to answer the prompt “The people from the city in which John Doe lives speak” with “Japanese”. More generally, suppose there are two factual associations, one from head entity a to bridge entity b , and one from bridge entity b to tail entity c . Two-hop reasoning requires the model to compose the two factual associations $a \rightarrow b$ and $b \rightarrow c$ together so that the model, when prompted with head entity a , recalls the tail entity c .

In two-hop reasoning, the novel fact can be in either the first hop ($a \rightarrow b$) or the second hop ($b \rightarrow c$), and we construct synthetic datasets to study both (Table 1). Concretely, the two datasets FIRST-HOP and SECOND-HOP are created from a set of 20 cities, each associated with a distinct language and landmark, as well as a set of 20 fictitious names. For each of the datasets, we randomly pair fictitious names with cities to populate fact and implication templates (Table 1). The key difference between the two datasets is that the FIRST-HOP contains the novel fact in the first hop in two-hop reasoning, and SECOND-HOP contains the novel fact in the second hop. We find that the OLMo-7b model is indeed capable of two-hop OCR for both datasets (Fig. 3).

4. Extractive structures framework

This section describes the extractive structures framework and proposes metrics for identifying extractive structures. Our framework models how weight changes influence behavior via an interplay between weights and activations, and is grounded in empirically measurable metrics.

Extractive structures model out-of-context reasoning as the coordination of three groups of components during the forward pass on the prompt p : the *informative components*, *upstream extractive components* and *downstream extractive components* (Fig. 1).

Informative components store the salient information about the newly learned facts as weight changes. While all components undergo weight changes during finetuning, only the weight changes in the informative components are important for correctly predicting the implications. In Fig. 1, informative components store the association “John Doe” \rightarrow “Tokyo” that is later used by the extractive components at test time.

Upstream extractive components parse the input prompt p to produce relevant intermediate activations as inputs to informative components. Upstream components are not importantly changed by finetuning, but are important for correctly activating the informative component at test time¹. In Fig. 1, upstream components produce the intermediate representation of “John Doe” that informative components convert to “Tokyo” using their newly stored associations.

Downstream extractive components process the outputs of informative components to produce the correct continuation a . In Fig. 1, downstream components look up the language of the city “Tokyo” to predict “Japanese”.

For each of the three groups of components (informative, upstream, downstream), we propose a metric to identify them. The metrics are based on causal interventions on the computational graph of the LM. For efficient computation, we linearly approximate the causal metrics with Grad-CAM style attribution scores (Selvaraju et al., 2017).

4.1. Causal metrics on the computational graph

We define metrics for extractive structures in terms of the LM’s computational graph. Denote the inputs and outputs of the LM as x and y . For example, for an implication (p, a) , x would be the prompt p , and y would be a probability distribution over possible answers. We measure whether the LM has correctly answered the prompt with a real-valued reward $\mathcal{R}(y, a)$ (e.g. log-probability of a). Thus, x is a leaf node and \mathcal{R} is the terminal node in the computational graph.

¹Weight changes are empirically often low-rank (Aghajanyan et al., 2020), and would therefore have no influence on component outputs unless component inputs fall in the right subspace.

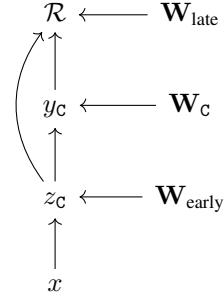


Figure 4. Computational graph of a LM, focusing on component C . All components in earlier and later layers are folded into $\mathbf{W}_{\text{early}}$ and \mathbf{W}_{late} respectively. The direct arrow from component input z_C to reward \mathcal{R} reflects the skip connection in transformers.

The internal nodes of the LM computational graph are the inputs and outputs to components in the LM. Following conventions in LM interpretability (Wang et al., 2022; Elhage et al., 2021), we define a component to be either an MLP or attention head at a specific layer and token position of the transformer. Formally, let C be a component in the LM, z_C and y_C be its input and output, \mathbf{W}_C be its weights, and f_C describe its computation so that $y_C = f_C(z_C, \mathbf{W}_C)$.

We simplify the full computational graph by focusing on a particular component C (Fig. 4). We denote the collective weights of components earlier and later than component C as $\mathbf{W}_{\text{early}}$ and \mathbf{W}_{late} , so the overall LM weights \mathbf{W} are represented by three leaf nodes $\mathbf{W}_{\text{early}}$, \mathbf{W}_C , and \mathbf{W}_{late} .

Using this computational graph, we can express precisely the causal effects we expect if component C is one of the three extractive structures defined above. We fix the input x and desired output a , and measure how the reward \mathcal{R} varies under certain interventions on the graph. We denote an intervention that sets the value of a node v to a counterfactual value v' with $v \leftarrow v'$, and the resulting reward as $\mathcal{R}[v \leftarrow v']$. We also denote the original pretrained weights as \mathbf{W} and the finetuned weights as \mathbf{W}' , and similarly denote node values in the finetuned model as their primed versions (e.g. z'_C).

Below we describe interventions that capture how each of the three structures mediate changes to the weights.

Informative components. Intuitively, an informative component contains the newly learned knowledge that the rest of the network extracts. Therefore, if component C is an informative component, we expect setting $\mathbf{W}_C \leftarrow \mathbf{W}'_C$ while leaving all other weights unchanged to improve the reward. We thus write the informative score for component C as:

$$\mathcal{I}_C = \mathcal{R}[\mathbf{W}_C \leftarrow \mathbf{W}'_C] - \mathcal{R} \quad (1)$$

Downstream components. Intuitively, a downstream com-

ponent processes the output containing the newly learned knowledge into useful output for the current prediction. Therefore, if component C is a downstream component, we expect its output y_C to help increase reward, but only if its input z_C contains the newly learned knowledge. We therefore compute the new z'_C with the new weights $\mathbf{W}'_{\text{early}}$ and contrast it with the original z_C . Specifically, we compute the downstream score for component C as:

$$\mathcal{D}_C = \mathcal{R}[y_C \leftarrow f_C(z'_C, \mathbf{W}_C)] - \mathcal{R} \quad (2)$$

Upstream components. Intuitively, an upstream component needs to process the input to appropriately query the informative component. Therefore, if component C is an upstream component, we expect its outputs to feed into later layers to increase reward, but only if the later layers contain the updated weights. The upstream score will thus be a difference in differences: one difference that measures the importance of component C for later layers, and another that measures the change from the old to the new weights.

A standard way of measuring importance of a node is to ablate its value by setting it to a constant, such as its mean value over some reference set (Chan et al., 2022). To evaluate the importance of component C , we set its output y_C to a constant value y_C^* and measure the decrease in reward. Formally, we define the importance of component C as

$$\mathcal{R}_C = \mathcal{R} - \mathcal{R}[y_C \leftarrow y_C^*]. \quad (3)$$

Upstream components have higher importance when future informative layers are updated to the new weights \mathbf{W}' . We therefore compute the upstream score for component C as the difference in the importance \mathcal{R}_C under the new weights $\mathbf{W}'_{\text{late}}$ and the old weights \mathbf{W}_{late} :

$$\mathcal{U}_C = (\mathcal{R}[\mathbf{W}_{\text{late}} \leftarrow \mathbf{W}'_{\text{late}}] - \mathcal{R}[\mathbf{W}_{\text{late}} \leftarrow \mathbf{W}'_{\text{late}}, y_C \leftarrow y_C^*]) - (\mathcal{R} - \mathcal{R}[y_C \leftarrow y_C^*]) \quad (4)$$

4.2. Linearizing the extractive scores

We linearize the extractive scores to obtain quantities easily computed by a few forward and backward passes (Selvaraju et al., 2017). Specifically, for any node v in the computational graph, we approximate

$$\mathcal{R}[v \leftarrow v_1] - \mathcal{R}[v \leftarrow v_2] \approx \frac{\partial \mathcal{R}}{\partial v}(v_1 - v_2),$$

where the derivative can be evaluated at either v_1 or v_2 . In practice, we choose v_1 or v_2 based on computational convenience (implementation details in Sec. B).

We additionally show in appendix A that the linearized scores can alternatively be derived as first-order perturbations to the importance (Eq. 3) of component C under perturbations to the weights \mathbf{W} . This suggests that the linearized scores ought to be comparable in magnitude.

5. Extractive structures in two-hop reasoning

We next use the extractive scores from the previous section to identify informative, upstream, and downstream components for the FIRST-HOP and SECOND-HOP datasets. Our results indicate that OCR in two-hop reasoning occurs by recalling each hop sequentially (Sec. 5.1). Moreover, we find that facts are stored redundantly across many LM layers, but early layers enable first-hop generalization while later layers enable second-hop generalization (Sec. 5.2). Our work suggests that understanding OCR mechanisms can help design interventions that determine generalization properties.

5.1. Extractive structures perform latent two-hop recall

As described in Sec. 3, two-hop reasoning requires the model to compose two factual associations $a \rightarrow b$ and $b \rightarrow c$ together so that the model recalls the tail entity c when prompted with head entity a (presumably by latently recalling the bridge entity b). One hypothesized mechanism for this is *latent two-hop* (Yang et al., 2024), which posits two groups of components: one responsible for the **first-hop recall** $a \rightarrow b$, and another for the **second-hop recall** $b \rightarrow c$.

If LMs use latent two-hop recall for OCR, we expect the extractive scores to correspond to the two groups of components. Because the FIRST-HOP and SECOND-HOP datasets introduce novel facts at different hops, we expect the extractive components to differ. Specifically, for the FIRST-HOP dataset where the novel fact is on the first hop, we expect the informative components to be the first-hop recall components, and the downstream components to include the second-hop recall components. In contrast, for the SECOND-HOP dataset where the novel fact is on the second hop, we expect the upstream components to include the first-hop recall components, and the informative components to be the second-hop recall components.²

Setup. We study an intermediate training checkpoint of OLMo-7b, taking the last checkpoint before the final annealing stage because annealing may interfere with finetuning (Ibrahim et al., 2024). For each dataset (FIRST-HOP and SECOND-HOP), we finetune the model on the facts and compute extractive scores on implications by comparing the finetuned weights with the pretrained weights. We provide more training details in Sec. C; in particular we often observe learning rate sensitivity (Sec. F), where OCR only occurs at certain learning rates; we thus focus on the learning rates for which OCR most reliably occurs.

²In the FIRST-HOP dataset, we expect downstream components to also include components that move information in the outputs of first-hop recall to the inputs of second-hop recall components. Similarly, we expect upstream structures for the SECOND-HOP dataset to capture the same information-moving components. We believe both FIRST-HOP downstream and SECOND-HOP upstream scores identify layer 26 attention heads for this role (Fig. 5).

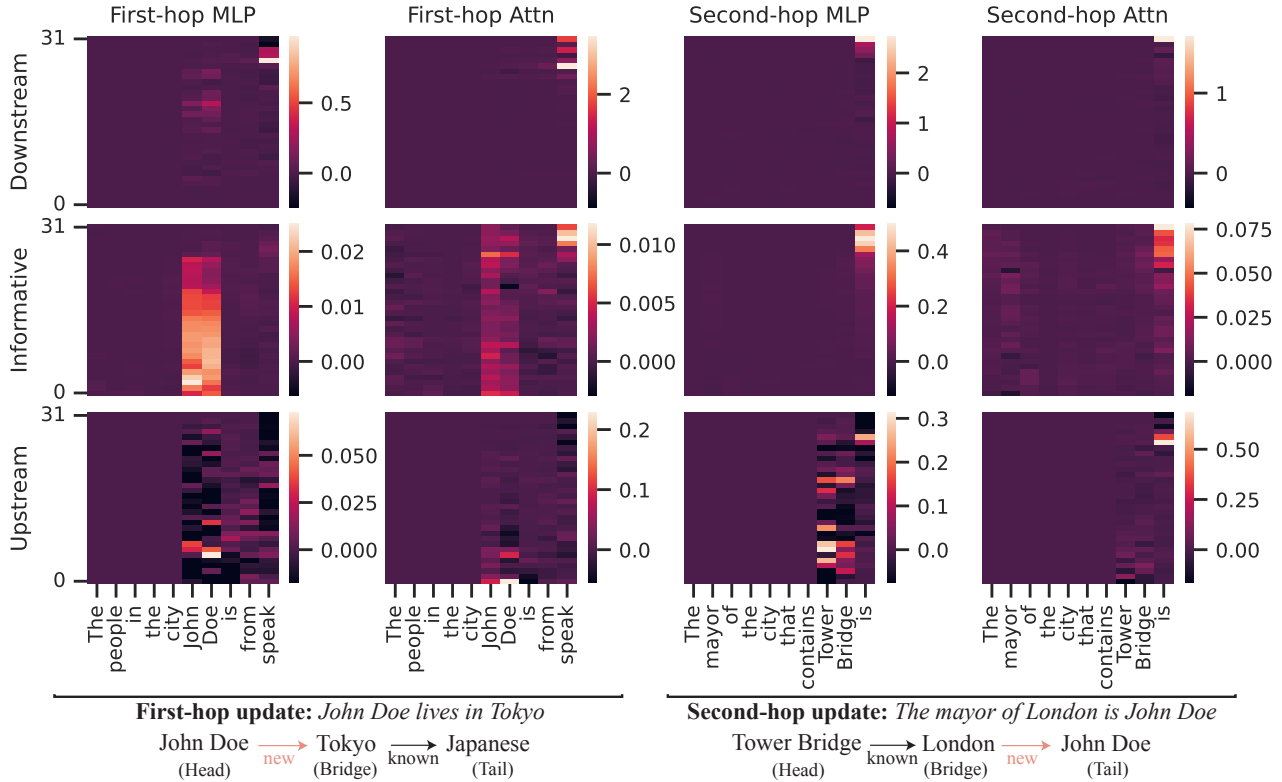


Figure 5. Extractive scores for the FIRST-HOP (left) and SECOND-HOP datasets (right). Scores are averaged over the dataset. Some entities are more than two tokens long; we visualize only the scores of their last two tokens. The attention scores are summed across all the attention heads that are outputting to the same position. The FIRST-HOP informative scores and SECOND-HOP upstream scores point to the early-middle MLPs at head entity tokens as the first-hop recall components. The FIRST-HOP downstream scores and SECOND-HOP informative scores point to the early-middle MLPs at the last token as the second-hop recall components.

Results. Our computed extractive scores are consistent with latent two-hop recall (Fig. 5). For the FIRST-HOP dataset, high informative scores are localized to the MLPs in early-middle layers of the head entity tokens (“John Doe”), which we interpret as the first-hop recall components. The downstream scores are localized to the late MLPs and attention heads at the last token, which we interpret as second-hop recall components. For the SECOND-HOP dataset, high upstream scores are localized to the early/middle MLPs of the head entity tokens (“Tower Bridge”), matching the first-hop recall components identified in the FIRST-HOP dataset. The informative scores are localized to the late MLP layers in the last token position, matching the second-hop recall components in FIRST-HOP.

These results from analyzing finetuning broadly reinforce findings from prior works that analyze pretrained models. Yang et al. (2024) and Biran et al. (2024) argued that first-hop recall occurs at the early-middle layers of the last head entity token, whereas the second-hop recall occurs at the late layers of the last token. Our extractive scores agree with both claims, except that we also find that both head entity tokens (e.g. “John” and “Doe”) store factual infor-

mation, and not just the last token. Moreover, while prior works (Geva et al., 2023; 2020; Meng et al., 2022) tend to study how MLPs store and recall facts and how attention heads move factual information, we find instead that attention heads can also store factual information. Specifically, the informative scores from both datasets indicate that the late attention heads at the last token position store some factual information. Overall, extractive scores complement conventional interpretability analysis on trained models by leveraging information in *weight changes*, and can verify known phenomena and discover new ones.

5.2. Different layers generalize differently

In this section we rigorously test an implication of the earlier extractive scores (Sec. 5.1): that storing facts in the early-middle layers enables first-hop updates, whereas storing in the late layers enables second-hop updates. Specifically, the informative scores (Fig. 5) show that weight changes to the early-middle MLP layers (first 24) are salient for the FIRST-HOP dataset, i.e. novel facts stored in the early-middle layers can be used as the first hop when composed with known second-hop facts. Conversely, weight changes to the late

Frozen Layers	FIRST-HOP		SECOND-HOP	
	Fact	Impl.	Fact	Impl.
None	0.00	0.00	0.00	1.80
Early	5.10	8.40	0.95	1.85
Late	0.00	0.00	0.10	6.30
All	9.20	9.25	9.10	9.50
Early (pre)	0.00	6.50	0.00	0.50
Late (pre)	0.00	0.10	0.00	6.60

Table 2. Mean ranks of facts and implications when freezing weights post-training or pre-training. Freezing early layers (first 24) harm first-hop OCR but not second-hop OCR, and vice versa for late layers (last 8). ‘None’ and ‘All’ are baselines where we use the full finetuned weights and original weights respectively.

MLP layers (last 8) are salient for the SECOND-HOP dataset, i.e. novel facts stored in the late layers can be used as the second hop when composed with known first-hop facts.

Note that when finetuning on facts, the model does not know whether the facts will later be used as the first hop or second hop in two-hop reasoning; we therefore expect the model to encode facts across all layers (both early-middle and late) to enable different forms of generalization.

To validate our hypothesis, we perform causal experiments where we freeze the weights on certain layers to the original pretrained weights and check if the model retains its knowledge of facts and implications. If the informative scores indeed correctly identified the salient weight changes in the model, we expect freezing the early-middle layers to hurt the implications for the FIRST-HOP dataset but not the SECOND-HOP dataset, and vice versa for the late layers.

Our results (Table 2) show that, compared to not freezing any layer (“None”), freezing the early-middle layers (“Early”) increases the mean rank for FIRST-HOP implications, but not for SECOND-HOP implications. Conversely, freezing the late layers (“Late”) increases the mean rank for SECOND-HOP implications but not for FIRST-HOP implications. Further, we find that freezing the early-middle layers partially increases the mean ranks for FIRST-HOP facts and SECOND-HOP facts, suggesting that when finetuning on all layers, facts are stored across all layers, but are disproportionately present in the early-middle layers.

We next show that facts can *in principle* be stored at both early-middle and late layers, but the choice of layer influences generalization. We now freeze either the early-middle or late layers *before* finetuning, and then re-finetune the remaining layers on the respective datasets. We expect to see that freezing either part should learn facts well, but as before would enable OCR for one dataset but not the other.

Our results (Table 2) show that freezing early-middle layers and re-finetuning the late layers (“Early (pre)”) still

harms FIRST-HOP implications while enabling SECOND-HOP implications, and vice versa for freezing late layers (“Late (pre)”). Moreover, facts are now reliably recalled in both settings. This supports the hypothesis that facts can be stored across many layers, but different layers enable different forms of generalization.

Our findings suggest that localization matter for knowledge editing, because it influences the generalization properties of the stored facts. Early knowledge editing works (Meng et al., 2022) suggested that facts are stored in a *specific* localized set of components, but later work (Hase et al., 2023) suggested that localization does not matter because facts can be edited at *any* point in the LM. Our results suggest that facts should be edited at *every* point in the LM to improve generalization.

6. Origins of extractive structures

We now turn our attention to how extractive structures are learned during pretraining. For OCR to occur, backpropagation on training facts must encode information in a way that is legible to the extractive structures at inference time; in other words, some mechanism must coordinate between facts encoded at training time and facts latently reasoned about at inference time.

We describe a mechanism during pretraining that solves the coordination problem between the backward pass and the extractive components. Suppose at a point during pretraining the model already knows a fact F (i.e. the earlier backward pass on F has already encoded it in the weights), and now encounters its implication Impl F. This could happen by chance from training data shuffling. To learn the implication Impl F, the model could either simply learn to memorize it, or, crucially, learn how to extract fact F from its weights and produce the implication Impl F. This creates a training signal for the formation of extractive structures that are adapted to how earlier facts have been encoded.

Our concrete hypothesis is thus that extractive structures are learned when encountering implications of already-known facts during training. We test two predictions of this hypothesis: a data ordering effect (Sec. 6.1) and a weight grafting effect (Sec. 6.2).

6.1. Data ordering

The hypothesis predicts a data ordering effect during pretraining, where if all the facts appear after their implications, then the model cannot learn extractive structures, and hence cannot later generalize to implications of new facts. Conversely, if all facts precede their implications, then extractive structures may form and later enable OCR.

The data ordering effect suggests a departure from the stan-

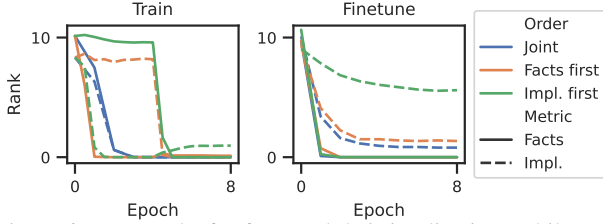


Figure 6. Mean ranks for facts and their implications while continued pretraining on training facts $\mathcal{F}_{\text{train}}$ (left), and while subsequently finetuning on test facts $\mathcal{F}_{\text{test}}$ (right). Compared to ‘Joint’ and ‘Facts first’, the ‘Implications first’ data order generalizes significantly worse to test implications when finetuned on test facts.

standard statistical machine learning view of optimization as model selection from a family. Instead, optimization is a dynamical process during which learning depends on the model’s internal state: whether the model learns extractive structures from implications depends on whether the model already knows the underlying facts.

Concretely, we study a controlled synthetic setup where a pretrained model is finetuned to learn a new form of implication. This finetuning process simulates what would have happened if the pretraining data had contained these novel implications. For clarity we call this phase *continued pretraining*. If continued pretraining successfully creates new extractive structures, we expect further finetuning the new model on new facts to generalize to their implications.

The new form of implications are derived from fictitious associations, whereas earlier implications are derived from known associations (e.g. “Tokyo” \rightarrow “Japanese”). Concretely, we assign random animals to cities (e.g. “Tokyo” \rightarrow “tiger”), and create fictitious relations “dax” and “wug” so that “John Doe dax Tokyo” implies “John Doe wug the tiger”. More generally, we create city-animal pairs $\{(c_i, a_i)\}$, and construct relations so that for any name n and city-animal pair (c_i, a_i) , “ n dax c_i ” implies “ n wug a_i ”.

Setup. We construct a train dataset of 80 facts $\mathcal{F}_{\text{train}}$ and their implications $\text{Impl } \mathcal{F}_{\text{train}}$, and a smaller test dataset of 20 facts $\mathcal{F}_{\text{test}}$ and their implications $\text{Impl } \mathcal{F}_{\text{test}}$. We first randomly pair 20 cities with 20 animals. The train facts and implications are formed by randomly assigning 80 fictitious names to the 20 city-animal pairs. We construct the test facts and implications similarly using 20 other fictitious names. We ensure that every city is represented in the test facts.

We run continued pretraining on the training facts and their implications $\mathcal{F}_{\text{train}} \cup \text{Impl } \mathcal{F}_{\text{train}}$ and test if data ordering affects the model’s ability to perform OCR on the test facts $\mathcal{F}_{\text{test}}$. Specifically, we investigate three orderings of the training data: facts-then-implications (‘Facts first’), implications-then-facts (‘Impl. first’), and a setting where facts and implications are shuffled together (‘Joint’). To evaluate OCR,

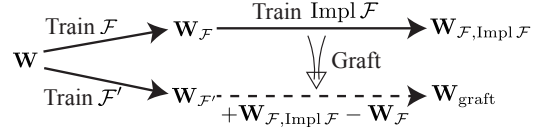


Figure 7. Visualization of grafting procedure. We hypothesize that the grafted weights contain extractive structures for the new form of implications, so that $\mathbf{W}_{\text{graft}}$ generalizes to $\text{Impl } \mathcal{F}'$.

we finetune the model on test facts $\mathcal{F}_{\text{test}}$, and measure its generalization to the test implications $\text{Impl } \mathcal{F}_{\text{test}}$.

Results. Figure 6 displays results for the OLMo-7b model from Sec. 5.1; see Sec G for results on additional models (Llama 3-8b, Gemma 2-9b, and Qwen 2-7b). Models continually pretrained on ‘Joint’ and ‘Facts-first’ exhibit significantly more out-of-context reasoning than for the ‘Impl-first’ data order (Fig. 6 right). This happens even though the model successfully learns the training facts and implications in all three data orderings (Fig. 6 left). This supports our hypothesis that extractive structures are learned when training on implications of already known facts.

Finally, the ‘Impl-first’ model exhibits a small amount of OCR generalization, since the implication mean rank decreases during finetuning (Fig. 6 right). This suggests an additional, unknown mechanism that contributes to OCR.

6.2. Weight grafting

In the data order where all facts precede implications, our hypothesis suggests that facts are learned in the first half of continued pretraining, and the extractive structures are learned in the second half. We therefore expect the change in weights between the middle and final checkpoints of continued pretraining to carry the extractive structures.

We test this by grafting this change in weights onto a model trained on counterfactual facts, and testing the model on counterfactual implications. For example, suppose “John Doe dax Tokyo” and “John Doe wug Tiger” are a fact and implication in the training dataset. If the change in weights carries the extractive structures that converts “Tokyo” to “Tiger”, then grafting this change in weights to a model counterfactually trained on “Jane Doe dax Tokyo” should generalize to “Jane Doe wug Tiger.” Concretely, our process is (Fig. 7):

1. Train on facts \mathcal{F} (the dax statements), to produce weights $\mathbf{W}_{\mathcal{F}}$
2. Train on implications $\text{Impl } \mathcal{F}$ (the wug statements) to produce weights $\mathbf{W}_{\mathcal{F}, \text{Impl } \mathcal{F}}$
3. Compute the difference in weights $\mathbf{W}_{\mathcal{F}, \text{Impl } \mathcal{F}} - \mathbf{W}_{\mathcal{F}}$
4. Train another copy of the model on counterfactual facts \mathcal{F}' to produce $\mathbf{W}_{\mathcal{F}'}$
5. Graft the weight difference over to produce the weights

Weights	Impl \mathcal{F}'	Impl \mathcal{F}	\mathcal{F}'
$\mathbf{W}_{\mathcal{F}'}$	9.13	8.55	0.00
$\mathbf{W}_{\text{graft}}$	1.13	3.30	0.10
$\mathbf{W}_{\text{control}}$	8.38	0.43	0.32

Table 3. Mean ranks for implications Impl \mathcal{F} , counterfactual implications Impl \mathcal{F}' , and counterfactual facts \mathcal{F}' for the model trained on counterfactual facts $\mathbf{W}_{\mathcal{F}'}$, grafted model $\mathbf{W}_{\text{graft}}$, and the control graft $\mathbf{W}_{\text{control}}$. The grafted model generalizes much better to counterfactual facts compared to the other two models.

$$\mathbf{W}_{\text{graft}} = \mathbf{W}_{\mathcal{F}'} + \mathbf{W}_{\mathcal{F}, \text{Impl } \mathcal{F}} - \mathbf{W}_{\mathcal{F}}$$

If our hypothesis is true, we expect the final model $\mathbf{W}_{\text{graft}}$ to generalize to counterfactual implications Impl \mathcal{F}' instead of the original implications Impl \mathcal{F} . We measure this by computing the mean rank of the implications as before.

Setup. We use the same train and test datasets as the data ordering experiment (Sec. 6.1), but additionally create a counterfactual version of the train dataset by re-assigning random cities/animals to the 80 names. We show results for the OLMo-7b model here, and others in Sec. G. As a control, we also graft the change in weights from training the model directly on the implications Impl \mathcal{F} , which we expect to only transfer implications and not counterfactual implications: $\mathbf{W}_{\text{control}} = \mathbf{W}_{\mathcal{F}'} + \mathbf{W}_{\text{Impl } \mathcal{F}} - \mathbf{W}$.

Results. We report results in Table 3. The weight graft $\mathbf{W}_{\text{graft}}$ lowers the mean rank for counterfactual implications Impl \mathcal{F}' from 9.13 to 1.13, versus 8.38 for the control. This suggests the weight graft contains extractive structures that can elicit counterfactual implications from counterfactual facts. The weight graft also transferred some of the original implications (mean rank 3.30), suggesting that when trained on implications, models partially memorize the implications in addition to learning extractive structures.

Overall, our weight grafting experiments directly identify the weights of the learned extractive structures, thereby supporting our hypothesis on how pretraining learns extractive structures. In Sec. E we further analyze these weights with extractive scores (Sec. 4) to show that the downstream extractive structures are indeed carried by the weight change. Our experiments demonstrate that extractive structures are a useful language for describing OCR training dynamics.

7. Conclusion

This work presents an in-depth analysis of how LMs can perform OCR in the two-hop reasoning task. We introduce extractive structures to describe how facts are encoded and recalled to predict implications, and empirically identify them in the OLMo-7b model. Additionally, we propose a hypothesis for how extractive structures are learned in

pretraining, and test two predictions of this hypothesis.

Our empirical results raise several immediate research questions. While the experiments in Sec. 6.1 hint at the possible existence of an alternative mechanism underlying OCR, its nature remains unclear. Furthermore, we have yet to fully characterize how the finetuning process depends on various hyperparameters and the pretrained model (Sec. F and G).

More broadly, we hope that extractive structures can lead to an underlying theory of generalization that captures the dynamical nature of optimization (Sec. 6.1). While our work focuses on two-hop reasoning, extractive structures could be a useful framework for analyzing other OCR tasks and provide conceptual grounding for this theory of generalization. Ultimately, identifying the principles and mechanisms behind OCR could offer insights into deep learning generalization, enabling the design of robust and safe machine learning systems.

Acknowledgements

We thank Amil Dravid, Alex Pan, Felix Binder, Owain Evans, Lijie Chen, and Alex Mallen for helpful feedback on the manuscript. JF acknowledges support from the OpenAI Superalignment Fellowship. JS was supported by the National Science Foundation under Grants No. 2031899 and 1804794. In addition, we thank Open Philanthropy for its support of both JS and the Center for Human-Compatible AI.

Impact Statement

This paper aims to deepen our understanding of empirical deep learning phenomena. We believe such understanding may potentially lead to stronger theories of deep learning generalization, which could help society develop and deploy deep learning systems more safely.

References

Aghajanyan, A., Zettlemoyer, L., and Gupta, S. Intrinsic dimensionality explains the effectiveness of language model fine-tuning. *arXiv preprint arXiv:2012.13255*, 2020.

Allen-Zhu, Z. and Li, Y. Physics of language models: Part 3.2, knowledge manipulation. *arXiv preprint arXiv:2309.14402*, 2023.

Balesni, M., Korbak, T., and Evans, O. The two-hop curse: LLMs trained on a- ζ b, b- ζ c fail to learn a- ζ c. *arXiv preprint arXiv:2411.16353*, 2024.

Berglund, L., Stickland, A. C., Balesni, M., Kaufmann, M., Tong, M., Korbak, T., Kokotajlo, D., and Evans, O. Taken

- out of context: On measuring situational awareness in llms. *arXiv preprint arXiv:2309.00667*, 2023a.
- Berglund, L., Tong, M., Kaufmann, M., Balesni, M., Stickland, A. C., Korbak, T., and Evans, O. The reversal curse: Llms trained on” a is b” fail to learn” b is a”. *arXiv preprint arXiv:2309.12288*, 2023b.
- Biran, E., Gottesman, D., Yang, S., Geva, M., and Globerson, A. Hopping too late: Exploring the limitations of large language models on multi-hop queries. *arXiv preprint arXiv:2406.12775*, 2024.
- Cammarata, N., Carter, S., Goh, G., Olah, C., Petrov, M., Schubert, L., Voss, C., Egan, B., and Lim, S. K. Thread: circuits. *Distill*, 5(3):e24, 2020.
- Chan, L., Garriga-Alonso, A., Goldowsky-Dill, N., Greenblatt, R., Nitishinskaya, J., Radhakrishnan, A., Shlegeris, B., and Thomas, N. Causal scrubbing: A method for rigorously testing interpretability hypotheses. In *AI Alignment Forum*, pp. 10, 2022.
- Chang, H., Park, J., Ye, S., Yang, S., Seo, Y., Chang, D.-S., and Seo, M. How do large language models acquire factual knowledge during pretraining? *arXiv preprint arXiv:2406.11813*, 2024.
- Cohen, R., Biran, E., Yoran, O., Globerson, A., and Geva, M. Evaluating the ripple effects of knowledge editing in language models. *Transactions of the Association for Computational Linguistics*, 12:283–298, 2024.
- Elhage, N., Nanda, N., Olsson, C., Henighan, T., Joseph, N., Mann, B., Askell, A., Bai, Y., Chen, A., Conerly, T., DasSarma, N., Drain, D., Ganguli, D., Hatfield-Dodds, Z., Hernandez, D., Jones, A., Kernion, J., Lovitt, L., Ndousse, K., Amodei, D., Brown, T., Clark, J., Kaplan, J., McCandlish, S., and Olah, C. A mathematical framework for transformer circuits. *Transformer Circuits Thread*, 2021. <https://transformer-circuits.pub/2021/framework/index.html>.
- Geva, M., Schuster, R., Berant, J., and Levy, O. Transformer feed-forward layers are key-value memories. *ArXiv*, abs/2012.14913, 2020. URL <https://api.semanticscholar.org/CorpusID:229923720>.
- Geva, M., Bastings, J., Filippova, K., and Globerson, A. Dissecting recall of factual associations in auto-regressive language models. *arXiv preprint arXiv:2304.14767*, 2023.
- Groeneveld, D., Beltagy, I., Walsh, P., Bhagia, A., Kinney, R., Tafjord, O., Jha, A. H., Ivison, H., Magnusson, I., Wang, Y., et al. Olmo: Accelerating the science of language models. *arXiv preprint arXiv:2402.00838*, 2024.
- Grosse, R., Bae, J., Anil, C., Elhage, N., Tamkin, A., Tajdini, A., Steiner, B., Li, D., Durmus, E., Perez, E., et al. Studying large language model generalization with influence functions. *arXiv preprint arXiv:2308.03296*, 2023.
- Hase, P., Bansal, M., Kim, B., and Ghandeharioun, A. Does localization inform editing? surprising differences in causality-based localization vs. *Knowledge Editing in Language Models*, 2023.
- Ibrahim, A., Thérien, B., Gupta, K., Richter, M. L., Anthony, Q., Lesort, T., Belilovsky, E., and Rish, I. Simple and scalable strategies to continually pre-train large language models. *arXiv preprint arXiv:2403.08763*, 2024.
- Kandpal, N., Deng, H., Roberts, A., Wallace, E., and Raffel, C. Large language models struggle to learn long-tail knowledge. In *International Conference on Machine Learning*, pp. 15696–15707. PMLR, 2023.
- Kingma, D. P. and Ba, J. Adam: A method for stochastic optimization. *arXiv preprint arXiv:1412.6980*, 2014.
- Kramár, J., Lieberum, T., Shah, R., and Nanda, N. Atp*: An efficient and scalable method for localizing llm behaviour to components. *arXiv preprint arXiv:2403.00745*, 2024.
- Meng, K., Bau, D., Andonian, A., and Belinkov, Y. Locating and editing factual associations in gpt. *Advances in Neural Information Processing Systems*, 35:17359–17372, 2022.
- Olah, C., Satyanarayan, A., Johnson, I., Carter, S., Schubert, L., Ye, K., and Mordvintsev, A. The building blocks of interpretability. *Distill*, 3(3):e10, 2018.
- Onoe, Y., Zhang, M. J., Padmanabhan, S., Durrett, G., and Choi, E. Can llms learn new entities from descriptions? challenges in propagating injected knowledge. *arXiv preprint arXiv:2305.01651*, 2023.
- Qin, J., Zhang, Z., Han, C., Li, M., Yu, P., and Ji, H. Why does new knowledge create messy ripple effects in llms? *arXiv preprint arXiv:2407.12828*, 2024.
- Selvaraju, R. R., Cogswell, M., Das, A., Vedantam, R., Parikh, D., and Batra, D. Grad-cam: Visual explanations from deep networks via gradient-based localization. In *Proceedings of the IEEE international conference on computer vision*, pp. 618–626, 2017.
- Treutlein, J., Choi, D., Betley, J., Anil, C., Marks, S., Grosse, R. B., and Evans, O. Connecting the dots: Llms can infer and verbalize latent structure from disparate training data. *arXiv preprint arXiv:2406.14546*, 2024.
- Vig, J., Gehrmann, S., Belinkov, Y., Qian, S., Nevo, D., Singer, Y., and Shieber, S. Investigating gender bias in

language models using causal mediation analysis. *Advances in neural information processing systems*, 33: 12388–12401, 2020.

Wang, B., Yue, X., Su, Y., and Sun, H. Grokked transformers are implicit reasoners: A mechanistic journey to the edge of generalization. *arXiv preprint arXiv:2405.15071*, 2024.

Wang, K., Variengien, A., Conmy, A., Shlegeris, B., and Steinhardt, J. Interpretability in the wild: A circuit for indirect object identification in gpt-2 small. *arXiv preprint arXiv:2211.00593*, 2022.

Yang, S., Gribovskaya, E., Kassner, N., Geva, M., and Riedel, S. Do large language models latently perform multi-hop reasoning? *arXiv preprint arXiv:2402.16837*, 2024.

Zhang, X., Li, M., and Wu, J. Co-occurrence is not factual association in language models. *arXiv preprint arXiv:2409.14057*, 2024.

Zhong, Z., Wu, Z., Manning, C. D., Potts, C., and Chen, D. Mquake: Assessing knowledge editing in language models via multi-hop questions. *arXiv preprint arXiv:2305.14795*, 2023.

A. Linearizing extractive scores

First, we linearize the three extractive scores (Eq. 1, 2, 4) to obtain³

$$\bar{U}_C = \left(\frac{\partial \mathcal{R}}{\partial y_C} [\mathbf{W}_{\text{late}} \leftarrow \mathbf{W}'_{\text{late}}] - \frac{\partial \mathcal{R}}{\partial y_C} \right) (y_C - y_C^*) \quad (5)$$

$$\bar{I}_C = \frac{\partial \mathcal{R}}{\partial \mathbf{W}_C} (\mathbf{W}'_C - \mathbf{W}_C) \quad (6)$$

$$\bar{D}_C = \frac{\partial \mathcal{R}}{\partial y_C} (f_C(z'_C, \mathbf{W}_C) - y_C). \quad (7)$$

For the upstream score \bar{U}_C , we choose y_C as the point to evaluate the derivative. For the informative and downstream scores, we choose the original points \mathbf{W}_C and y_C respectively.

A.1. Linearized scores as perturbations

We shall show that the three linearized scores can be derived as terms in a first order perturbation to a single quantity. Specifically, consider a small perturbation to the weights $\delta \mathbf{W} = \mathbf{W}' - \mathbf{W}$. Let $\check{y}_C = \frac{\partial \mathcal{R}}{\partial y_C}$ for convenience. Keeping only first order terms, the three linearized extractive scores become

$$\bar{U}_C = \left(\frac{\partial \check{y}_C}{\partial \mathbf{W}_{\text{late}}} \delta \mathbf{W}_{\text{late}} \right) (y_C - y_C^*) \quad (8)$$

$$\bar{I}_C = \frac{\partial \mathcal{R}}{\partial \mathbf{W}_C} \delta \mathbf{W}_C \quad (9)$$

$$\bar{D}_C = \check{y}_C \nabla_{z_C} f_C(z_C, \mathbf{W}_C) \delta z_C \quad (10)$$

Consider the importance of component C (Eq. 3)

$$\mathcal{R}_C = \mathcal{R} - \mathcal{R}[y_C \leftarrow y_C^*].$$

Its linearization, evaluating \check{y}_C at y_C , is

$$\bar{\mathcal{R}}_C = \check{y}_C (f_C(z_C, \mathbf{W}_C) - y_C^*). \quad (11)$$

We shall show that under a small perturbation $\delta \mathbf{W}$, the first order terms in $\delta \bar{\mathcal{R}}_C$ contain the three extractive scores. By straightforward product rule, we have:

$$\delta \bar{\mathcal{R}}_C = \delta \check{y}_C (f_C(z_C, \mathbf{W}_C) - y_C^*) + \check{y}_C (\nabla_{\mathbf{W}_C} f_C(z_C, \mathbf{W}_C) \delta \mathbf{W}_C) + \check{y}_C (\nabla_{z_C} f_C(z_C, \mathbf{W}_C) \delta z_C).$$

We claim that the second and third terms are exactly the linearized informative score and downstream score, to the first order (Eq. 9, 10). However, first term is related to, but not exactly the linearized upstream score.

The third term is manifestly the downstream score (Eq. 10). To show that the second term is the linearized informative score (Eq. 9), we simply apply the chain rule to $\frac{\partial \mathcal{R}}{\partial \mathbf{W}_C}$ to obtain:

$$\begin{aligned} \bar{I}_C &= \frac{\partial \mathcal{R}}{\partial \mathbf{W}_C} \delta \mathbf{W}_C \\ &= \check{y}_C \nabla_{\mathbf{W}_C} f_C(z_C, \mathbf{W}_C) \delta \mathbf{W}_C. \end{aligned}$$

The first term is subtly different from the first-order linearized upstream score (Eq. 8). Denote the first term as

$$\bar{U}_C^* = \delta \check{y}_C (f_C(z_C, \mathbf{W}_C) - y_C^*). \quad (12)$$

³The linearized informative score is related to component-wise influence functions (Grosse et al., 2023).

Compared to the first-order linearized upstream score (Eq. 8), the first term contains $\delta\check{y}$ instead of $\frac{\partial\check{y}_c}{\partial\mathbf{W}_{\text{late}}}\delta\mathbf{W}_{\text{late}}$. To understand the difference, recall that according to the computation graph (Fig. 4), \mathcal{R} is dependent on z_c , \mathbf{W}_{late} , and y_c , and therefore so is \check{y}_c . Therefore, the term $\delta\check{y}_c$ may be expanded as:

$$\delta\check{y}_c = \frac{\partial\check{y}_c}{\partial\mathbf{W}_{\text{late}}}\delta\mathbf{W}_{\text{late}} + \frac{\partial\check{y}_c}{\partial z_c}\delta z_c + \frac{\partial\check{y}_c}{\partial y_c}\delta y_c.$$

The first term is exactly the term from the first-order linearized upstream score (Eq. 8). We can interpret \check{y}_c as the linearized form of what the subsequent layers do to process y_c . The first term therefore captures how the subsequent layers depends on the weight perturbation $\delta\mathbf{W}_{\text{late}}$, which is what the upstream score aims to capture. The second and third terms reflect the dependency of the subsequent layers on z_c and y_c , which describe modulatory effects that weight changes in earlier layers $\delta\mathbf{W}_{\text{early}}$ and \mathbf{W}_c have on how the late layers process y_c .

To summarize, the linearized importance of component C, under a small perturbation $\delta\mathbf{W}$, can be written:

$$\begin{aligned}\bar{\mathcal{R}}_c &= \bar{U}_c^* + \bar{I}_c + \bar{D}_c \\ &= \bar{U}_c + \bar{I}_c + \bar{D}_c + \frac{\partial\check{y}_c}{\partial z_c}(y_c - y_c^*)\delta z_c + \frac{\partial\check{y}_c}{\partial y_c}(y_c - y_c^*)\delta y_c\end{aligned}$$

B. Implementing extractive scores

In this section, we describe how we implement the extractive scores. By caching activations in the forward pass and gradients in the backward pass, we can efficiently compute the linearized extractive scores (Sec A). Importantly, while the linearized informative score and downstream score can be computed efficiently, the linearized upstream score cannot. We instead use a surrogate quantity that is efficient to compute.

B.1. Choice of reward

We use the log probability of the first token of the continuation, conditioned on the prompt, as the reward. All of our datasets have the property that the continuations have unique first tokens.

B.2. Computing informative score

The linearized informative score (Eq. 6) can be computed with one forward and one backward pass. Recall

$$\bar{I}_c = \frac{\partial\mathcal{R}}{\partial\mathbf{W}_c}(\mathbf{W}'_c - \mathbf{W}_c).$$

To compute this, can we perform a backward pass on the original weights \mathbf{W} , cache the gradient $\frac{\partial\mathcal{R}}{\partial\mathbf{W}_c}$ for every component C, and multiply by the component's corresponding weight change ($\mathbf{W}'_c - \mathbf{W}_c$).

B.3. Computing downstream score

The linearized downstream score (Eq. 7) can be computed with three forward passes and one backward pass. Recall

$$\bar{D}_c = \frac{\partial\mathcal{R}}{\partial y_c}(f_c(z'_c, \mathbf{W}_c) - y_c).$$

The steps are:

1. Run the model on the original weights \mathbf{W} and cache values of y_c for every component C
2. Run the backward pass to obtain the derivative $\frac{\partial\mathcal{R}}{\partial y_c}$
3. Run the model on new weights \mathbf{W}' to obtain cached values of z'_c
4. Compute $f_c(z'_c, \mathbf{W}_c)$, and thus \bar{D}_c . The computation in this step required is roughly the same as a forward pass.

B.4. Computing upstream score

The linearized upstream score (Eq. 5) cannot be computed with a constant number of forward/backward passes. Recall that

$$\bar{U}_c = \left(\frac{\partial\mathcal{R}}{\partial y_c}[\mathbf{W}_{\text{late}} \leftarrow \mathbf{W}'_{\text{late}}] - \frac{\partial\mathcal{R}}{\partial y_c}\right)(y_c - y_c^*).$$

The reason is that computing $\frac{\partial \mathcal{R}}{\partial y_C} [\mathbf{W}_{\text{late}} \leftarrow \mathbf{W}'_{\text{late}}]$ requires recomputing the every late layer in \mathbf{W}_{late} for every different component C . However, it turns out that a slightly different quantity can be computed efficiently:

$$\bar{U}_C^* = \left(\frac{\partial \mathcal{R}}{\partial y_C} [\mathbf{W}_{\text{late}} \leftarrow \mathbf{W}'_{\text{late}}, y_C \leftarrow y'_C, z_C \leftarrow z'_C] - \frac{\partial \mathcal{R}}{\partial y_C} \right) (y_C - y_C^*). \quad (13)$$

The derivative $\frac{\partial \mathcal{R}}{\partial y_C} [\mathbf{W}_{\text{late}} \leftarrow \mathbf{W}'_{\text{late}}, y_C \leftarrow y'_C, z_C \leftarrow z'_C]$ can be computed simply by running a forward and a backward pass on the new weights \mathbf{W}' .

In addition, this version of the upstream score is exactly the first perturbation term (Eq. 12) of the linearized importance discussed in Sec. A.

Therefore, for computation efficiency we use \bar{U}_C^* as a surrogate for \bar{U}_C . The steps to compute \bar{U}_C^* are thus:

1. Run the model on the original weights to compute y_C
2. Run the backward pass to compute $\frac{\partial \mathcal{R}}{\partial y_C}$
3. Run the model on the new weights \mathbf{W}' to compute $\frac{\partial \mathcal{R}}{\partial y_C} [\mathbf{W}_{\text{late}} \leftarrow \mathbf{W}'_{\text{late}}, y_C \leftarrow y'_C, z_C \leftarrow z'_C]$
4. Compute \bar{U}_C^* . The computation in this step required is roughly the same as a forward pass.

There remains one more detail: the choice for the baseline value y_C^* . We choose to perform a mean ablation, so that y_C^* is the average value of y_C across the dataset. To align token positions between input prompts containing entities of varying length, we assume all entities are two tokens long. In cases where entities have more than two tokens, we drop activations from all but the last two entity tokens. We check that no entities have fewer than two tokens.

C. Training details

Model. We primarily use the OLMo-7b-0424 model, step 477000. This is the last intermediate checkpoint before the final annealing phase during which the learning rate is decayed to zero.

Training. Throughout the paper, we finetune the model using the standard cross-entropy loss. We only include the loss on answer tokens. We freeze the embedding and unembedding layers. We use the Adam optimizer (Kingma & Ba, 2014) for 8 epochs at 3×10^{-6} learning rate, momentum (0.9, 0.999), and batch size 8. We find that OCR is sensitive to learning rates, as explored in Sec. F.

D. Dataset details

D.1. FIRST-HOP and SECOND-HOP dataset

The FIRST-HOP and SECOND-HOP datasets are composed from a list of 20 fictitious names, and a list of 20 city-language or city-landmark pairs. These are generated from Claude-3.5-sonnet. Here are they:

Grace,Miller
 Ethan,Parker
 Olivia,Hughes
 Jacob,Turner
 Ava,Stewart
 Noah,Clark
 Emma,Howard
 Liam,Bennett
 Mia,Sanders
 Lucas,Foster
 Sophia,Hayes
 Mason,Brooks
 Lily,Cooper
 Jackson,Bell
 Amelia,Ward
 Caleb,Bryant
 Chloe,Campbell
 Henry,Morgan
 Ella,Adams
 Owen,Foster

Tokyo,Japan,Japanese,Senso-ji Temple
 Beijing,China,Mandarin,Forbidden City
 Mumbai,India,Marathi,Gateway of India
 Paris,France,French,Eiffel Tower
 Berlin,Germany,German,Brandenburg Gate
 Moscow,Russia,Russian,St. Basil’s Cathedral
 Cairo,Egypt,Arabic,Great Pyramid of Giza
 Bangkok,Thailand,Thai,Wat Arun
 Istanbul,Turkey,Turkish,Blue Mosque
 Sao Paulo,Brazil,Portuguese,Ibirapuera Park
 Seoul,South Korea,Korean,N Seoul Tower
 Rome,Italy,Italian,Colosseum
 London,United Kingdom,English,Tower Bridge
 Madrid,Spain,Spanish,Plaza Mayor
 Athens,Greece,Greek,Acropolis
 Hanoi,Vietnam,Vietnamese,Ho Chi Minh Mausoleum
 Addis Ababa,Ethiopia,Amharic,Meskel Square
 Jakarta,Indonesia,Indonesian,Istiqlal Mosque
 Tehran,Iran,Persian,Azadi Tower
 Nairobi,Kenya,Swahili,Uhuru Gardens

For the FIRST-HOP dataset, we apply the following templates:

1. Facts: “[Name] lives in”, “[city]”
2. Implications: “The people in the city [Name] is from speak”, “[language]”

For the SECOND-HOP dataset, we apply the following templates:

1. Facts: “The mayor of [city] is”, “[Name]”
2. Implications: “The mayor of the city that contains [landmark] is”, “[Name]”

D.2. Fictitious implications

In Sec. 6, we introduced a new dataset with fictitious relations. This requires a pairing between cities and a list of animals. We use the same set of cities from before, and use the set of 20 animals that Zhang et al. (2024) generated.

We apply the following templates:

1. Facts: “[Name] dax”, “[city]”
2. Implications: “[Name] zong is the”, “[animal]”

Below are the 100 names and the 20 animals. The first 80 names are used for training, and the last 20 are used for testing.

Grace,Miller Ethan,Parker Olivia,Hughes Jacob,Turner Ava,Stewart Noah,Clark Emma,Howard Liam,Bennett Mia,Sanders Lucas,Foster Sophia,Hayes Mason,Brooks Lily,Cooper Jackson,Bell Amelia,Ward Caleb,Bryant Chloe,Campbell Henry,Morgan Ella,Adams Owen,Foster Abigail,King Samuel,White Zoe,Mitchell Nathan,Carter Leah,Scott	Elijah,Morris Madeline,Evans Daniel,Gray Hannah,Reed Cameron,Perry Natalie,Bryant Isaac,Peterson Violet,Phillips Dylan,Rogers Charlotte,Brooks Landon,Harris Avery,Jenkins Evan,Parker Maya,Nelson Connor,Green Sydney,Barnes Julian,Bennett Kaitlyn,Ross Logan,Foster Brooke,Adams Eli,Sanders Molly,Cooper Wyatt,Lee Tessa,Collins Blake,Roberts	Madison,Reed Andrew,Miller Hailey,Henderson Matthew,Foster Sophie,Lawson Benjamin,Williams Isabella,Baker Carter,James Layla,Murphy Brayden,Collins Gabriella,Foster Aiden,Peterson Audrey,Jenkins Joshua,Barnes Scarlett,Turner Ryan,Brooks Aubrey,Hayes Christopher,Bryant Harper,Bell Jason,Mitchell Madelyn,Phillips David,Harris Nora,Rogers Adam,Campbell Elise,Ward	Kevin,White Lucy,Stewart Brandon,Green Bella,Parker Christian,Clark Clara,Cooper Tyler,King Caroline,Morgan Jordan,Adams Stella,Scott Hunter,Morris Peyton,Lee Alex,Evans Elena,Carter Ian,Foster Autumn,Gray Jeremy,Bennett Lillian,Ross Nolan,Reed Morgan,Howard Gavin,Perry Paige,Turner Adrian,Williams Cora,Jenkins Parker,Bryant	lion tiger elephant giraffe zebra rhinoceros crocodile cheetah antelope ostrich monkey penguin koala dolphin jellyfish king snake butterfly turtle beaver squirrel
--	--	--	--	---

E. Localizing extractive structures in weight grafting

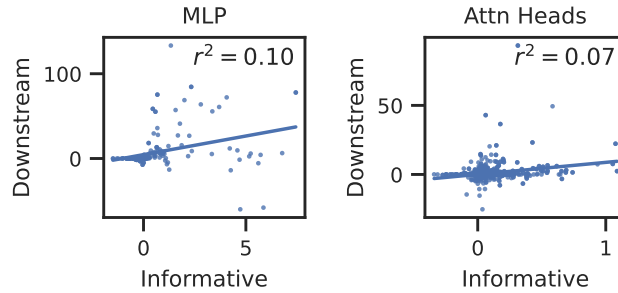


Figure 8. Correlation between downstream extractive scores and informative scores for MLPs (left) and attention heads (right).

Earlier in Sec. 6.2 we showed that a certain weight change contained newly learned extractive structures. In this section, we aim to identify the components that are modified by this weight change, and show that they are exactly the downstream extractive structures.

To identify the components modified by the weight change, we use the informative score. Consider the model finetuned on counterfactual train facts $\mathbf{W}_{\mathcal{F}'_{\text{train}}}$, and a reward defined based on how much the model knows the counterfactual train implications $\text{Impl } \mathcal{F}'_{\text{train}}$. Initially, the reward is low because the model only knows the counterfactual train facts \mathcal{F}' but not the train implications $\text{Impl } \mathcal{F}'_{\text{train}}$. Suppose that after grafting, the model $\mathbf{W}_{\text{graft}}$ can now predict counterfactual facts $\mathcal{F}'_{\text{train}}$ so that the reward is now high. Then, the informative scores with respect to this change in weights $\mathbf{W}_{\text{graft}} - \mathbf{W}_{\mathcal{F}'_{\text{train}}}$ would identify the important components modified by the weight change, because the informative scores identify components that, under the weight change, contribute to increasing the reward.

To show that these identified components are the downstream extractive structures, we apply the downstream scores to a different weight change. This time, consider the grafted model $\mathbf{W}_{\text{graft}}$. If we finetune this weights on test facts $\mathcal{F}_{\text{test}}$, then the resulting model should perform well on the test implications $\mathcal{F}_{\text{test}}$. The downstream score of this finetuning process should capture the downstream extractive structures that predicts corresponding animals from the cities recalled latently.

We compute the informative and downstream scores for the two weight changes described, and correlate the two approaches for localizing them (Fig. 8). We find that for both MLP components and attention heads, there is a statistically significant positive correlation between the two metrics. However, the Pearson correlation is small, suggesting that the two metrics do not align perfectly.

F. Learning rate sensitivity

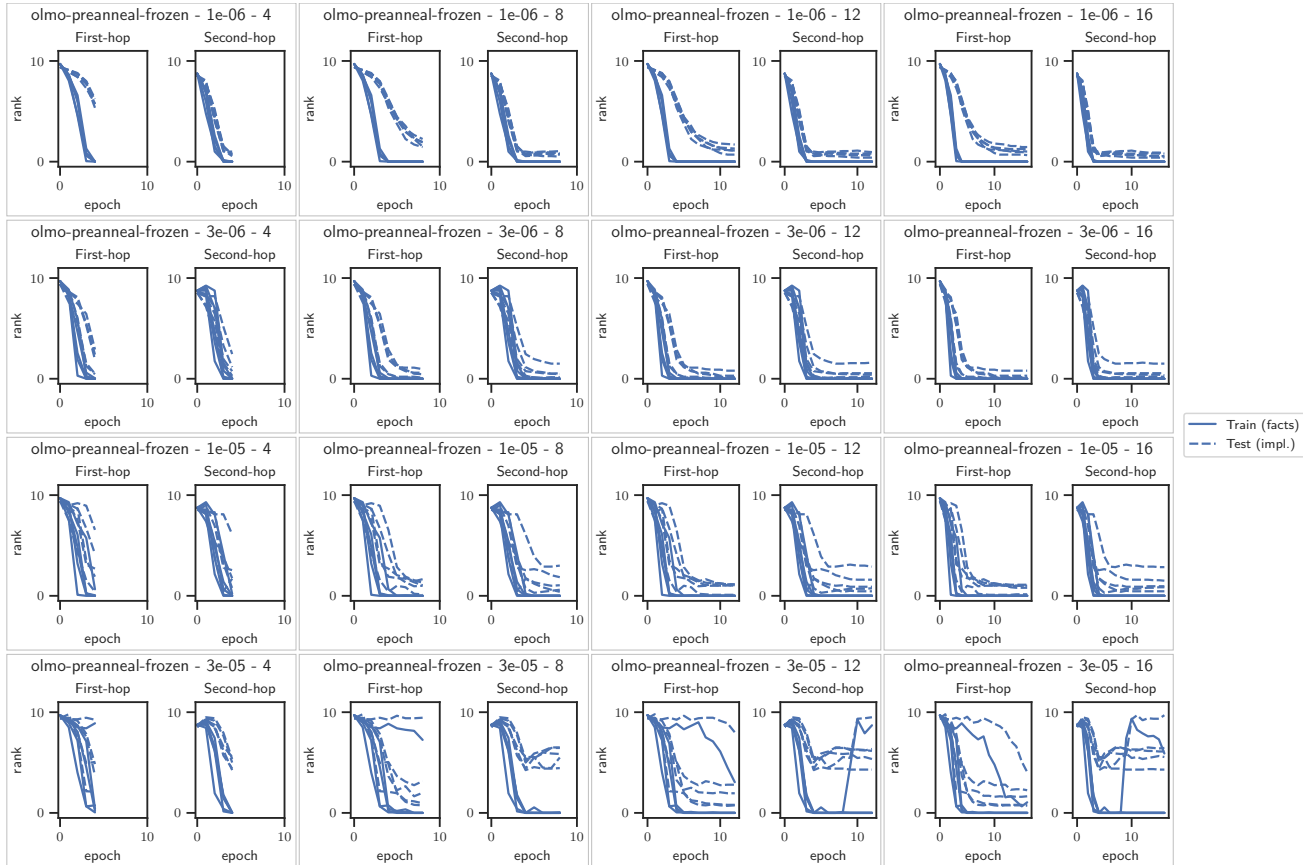


Figure 9. Two-hop OCR performance across different learning rates and epochs for the OLMo-7B pre-anneal checkpoint. 5 random seeds were used. The title has the format “model - lr - epochs”

We observe that the OCR ability exhibits learning rate sensitivity (Fig. 9). For both learning rates 1e-5 and 3e-6, we observe that the model appears to converge in train rank, but the test rank for 1e-5 is significantly higher than for learning rate 3e-6.

Similarly, data ordering and weight grafting effects are sensitivity to learning rates (Fig. 10, 11). Further, because whether or not extractive structures are learned in continued pretraining depends on the number of epochs of continued pretraining, the OCR performance also depends strongly on the number of epochs. Nonetheless, in most settings we do observe the expected qualitative pattern: that ‘Impl-first’ data ordering is worse than ‘Fact-first’ or ‘Joint’ at OCR, and that W_{graft} transfers counterfactual implications but not the control graft W_{control} .

G. Other models

In this section, we show three plots for three models. The three plots are on two-hop OCR performance, data ordering effect, and weight grafting effect. The three models are Llama-3-8b, Gemma-2-9B, and Qwen-2-7B. As in Sec. F, we sweep across learning rates and epochs, and try 5 random seeds.

Overall, the other models exhibit the same qualitative effects, but the effects are weaker and more sensitive to hyperparameters than in OLMo. We believe that it will be interesting to analyze properties of the models make them less good at OCR.

Extractive Structures Learned in Pretraining Enable Generalization on Finetuned Facts

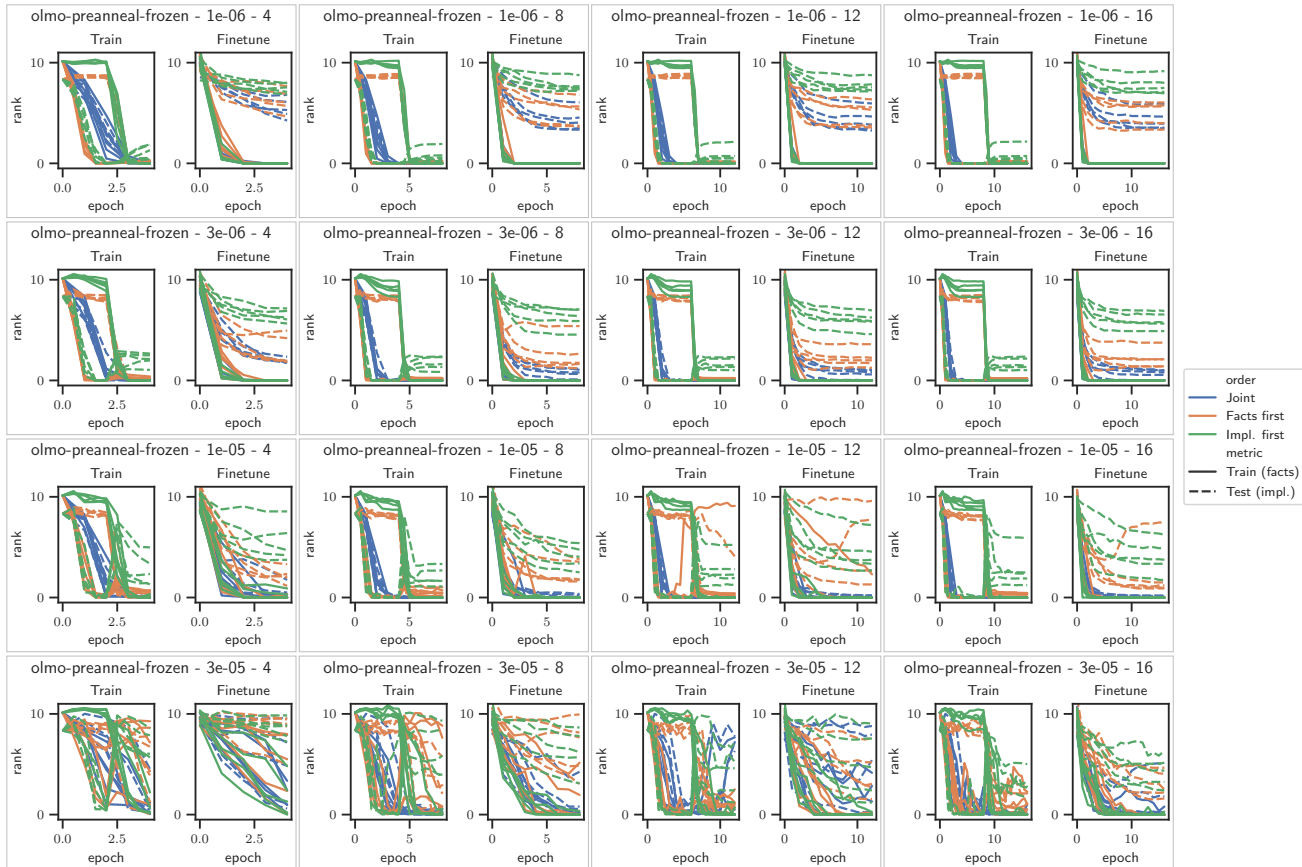


Figure 10. Data ordering effect across different learning rates and epochs for the OLMo-7B pre-anneal checkpoint. 5 random seeds were used. The title has the format “model - lr - epochs”

Two-hop OCR. (Figs. 12, 13, 14) We find that different models require different learning rates to exhibit OCR. All models can perform OCR on the FIRST-HOP dataset on some learning rate values. Performance is worse on SECOND-HOP dataset, but the mean rank does decrease significantly across all seeds.

Data ordering. (Figs. 15, 16, 17) We observe that ‘Fact-first’ exhibits greater or similar OCR compared with ‘Impl-first’, suggesting that the data ordering effect is present. For some settings, both ‘Fact-first’ and ‘Impl-first’ data orderings have similar, but non-trivial, OCR performance, which again points at the existence of an unknown alternate mechanism for learning extractive structures.

Weight grafting. (Figs. 18, 19, 20) All models, under the weight graft $\mathbf{W}_{\text{graft}}$, for an appropriate choice of hyperparameters, can predict counterfactual implications. However, in these models the weight graft also transfers the original implications, reinforcing the hypothesis that these models perform OCR less effectively, and instead memorize more.

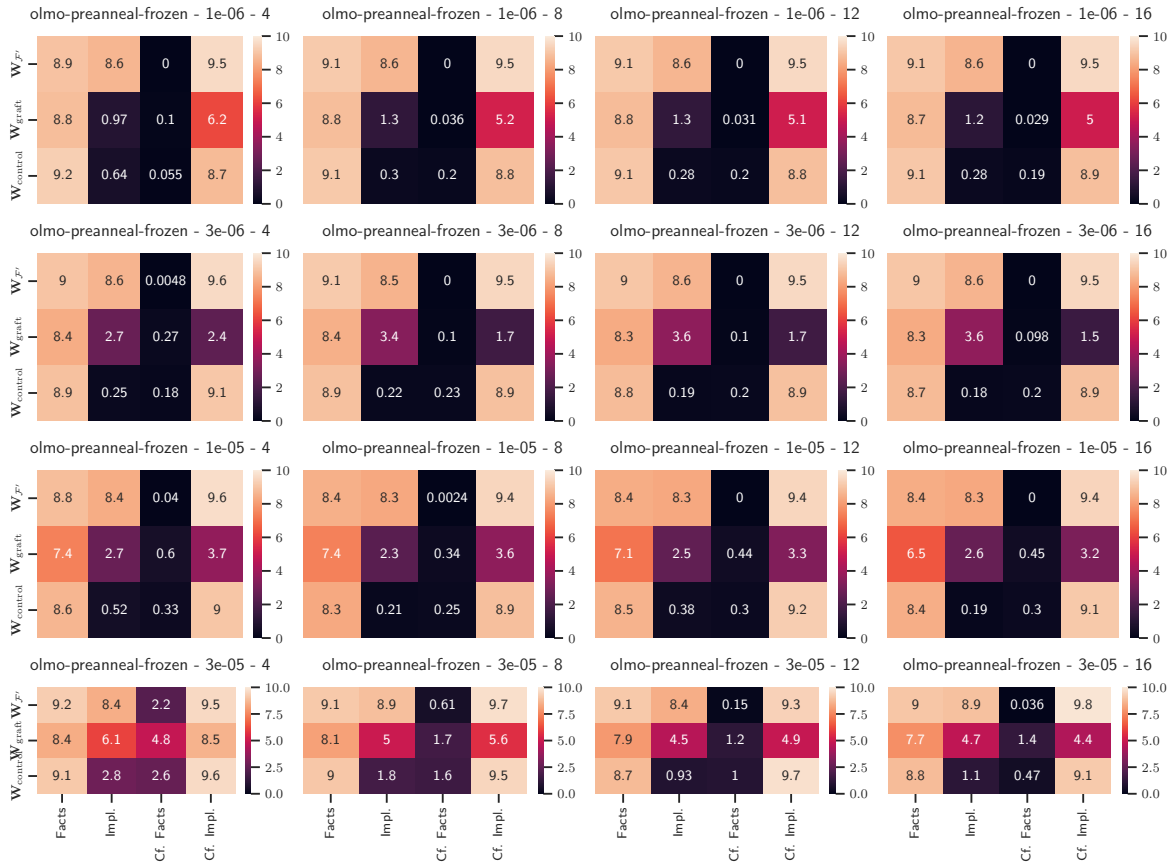


Figure 11. Weight grafting effect across different learning rates and epochs for the OLMo-7B pre-anneal checkpoint. 5 random seeds were used. We show the average mean rank across the 5 random seeds. The title has the format “model - lr - epochs”

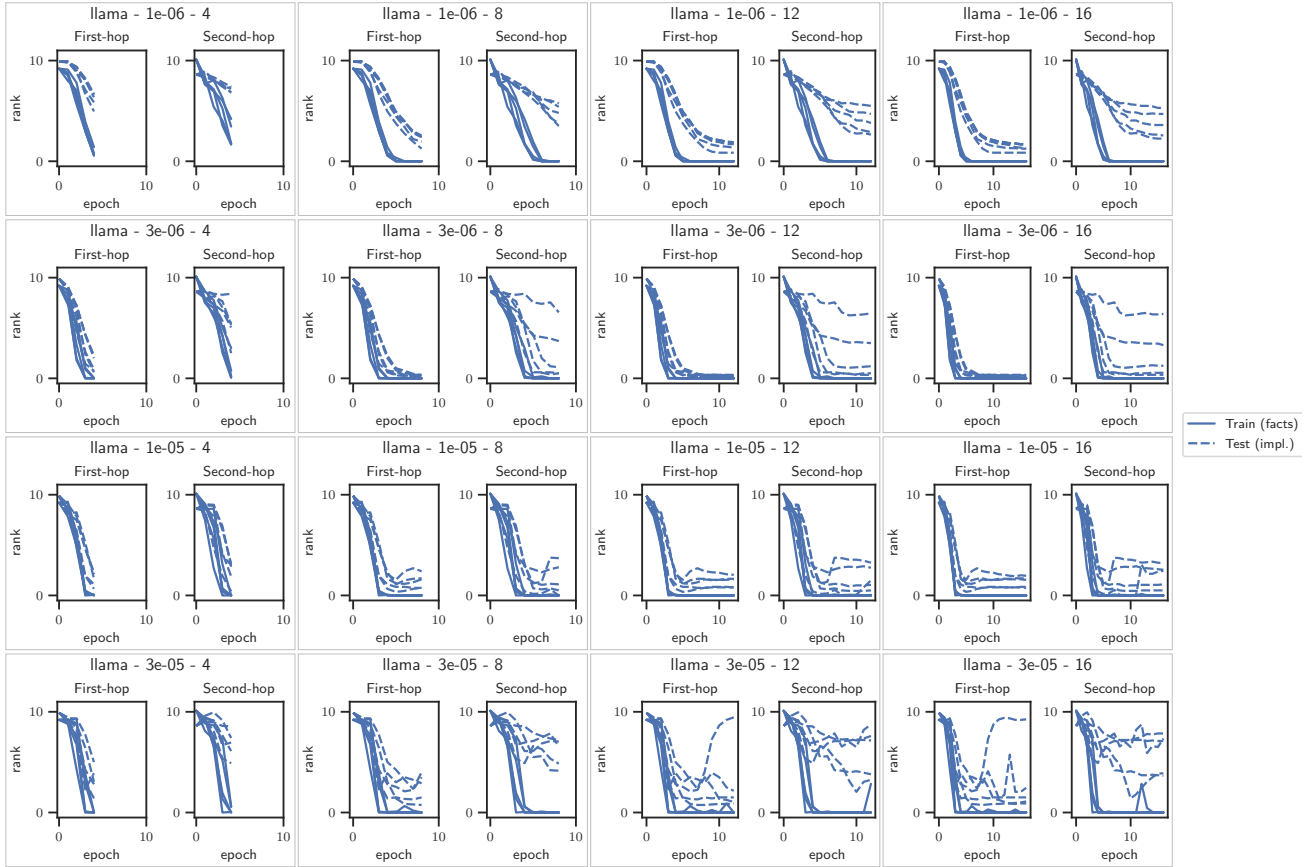


Figure 12. Two-hop OCR performance across different learning rates and epochs for Llama-3-8b. 5 random seeds were used. The title has the format “model - lr - epochs”

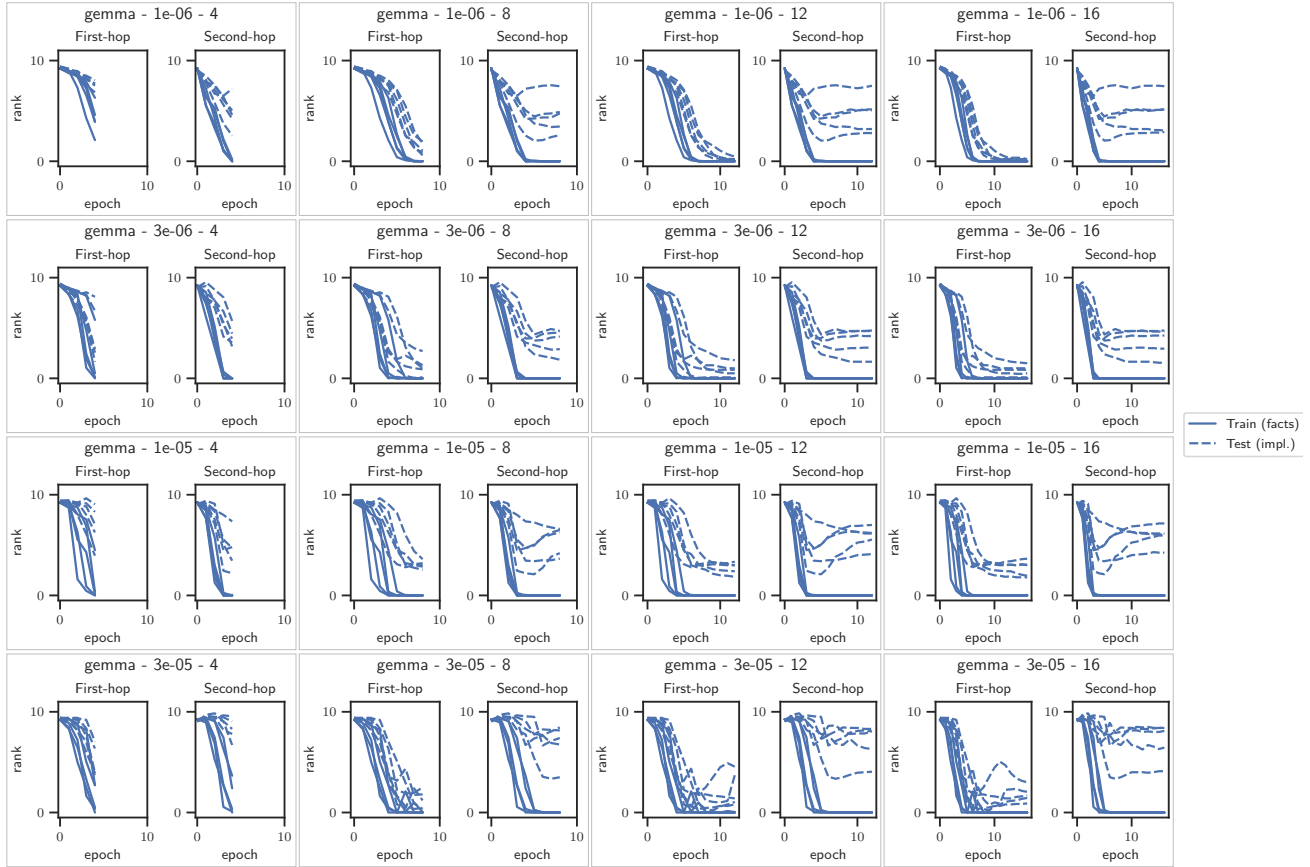


Figure 13. Two-hop OCR performance across different learning rates and epochs for Gemma-2-9B. 5 random seeds were used. The title has the format “model - lr - epochs”

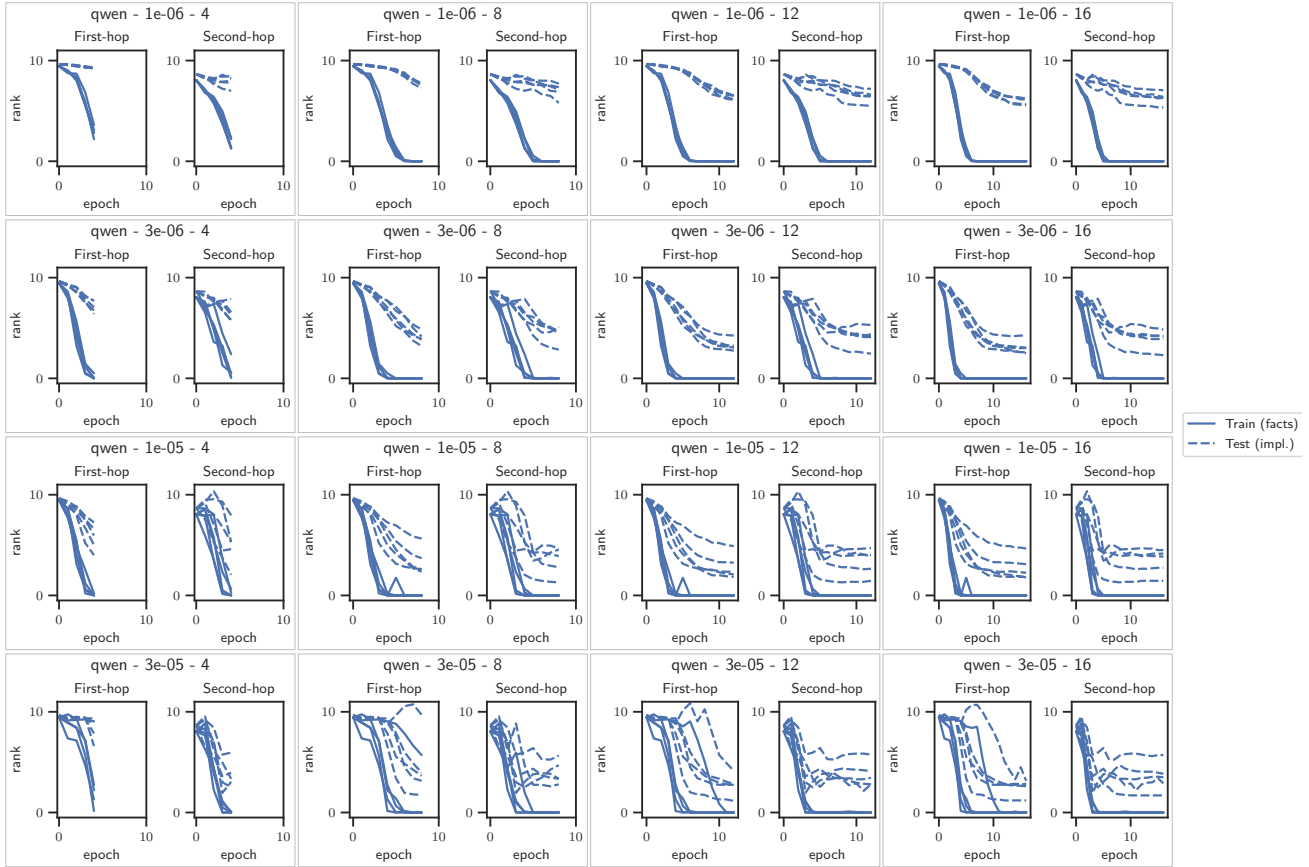


Figure 14. Two-hop OCR performance across different learning rates and epochs for Qwen-2-7B. 5 random seeds were used. The title has the format “model - lr - epochs”

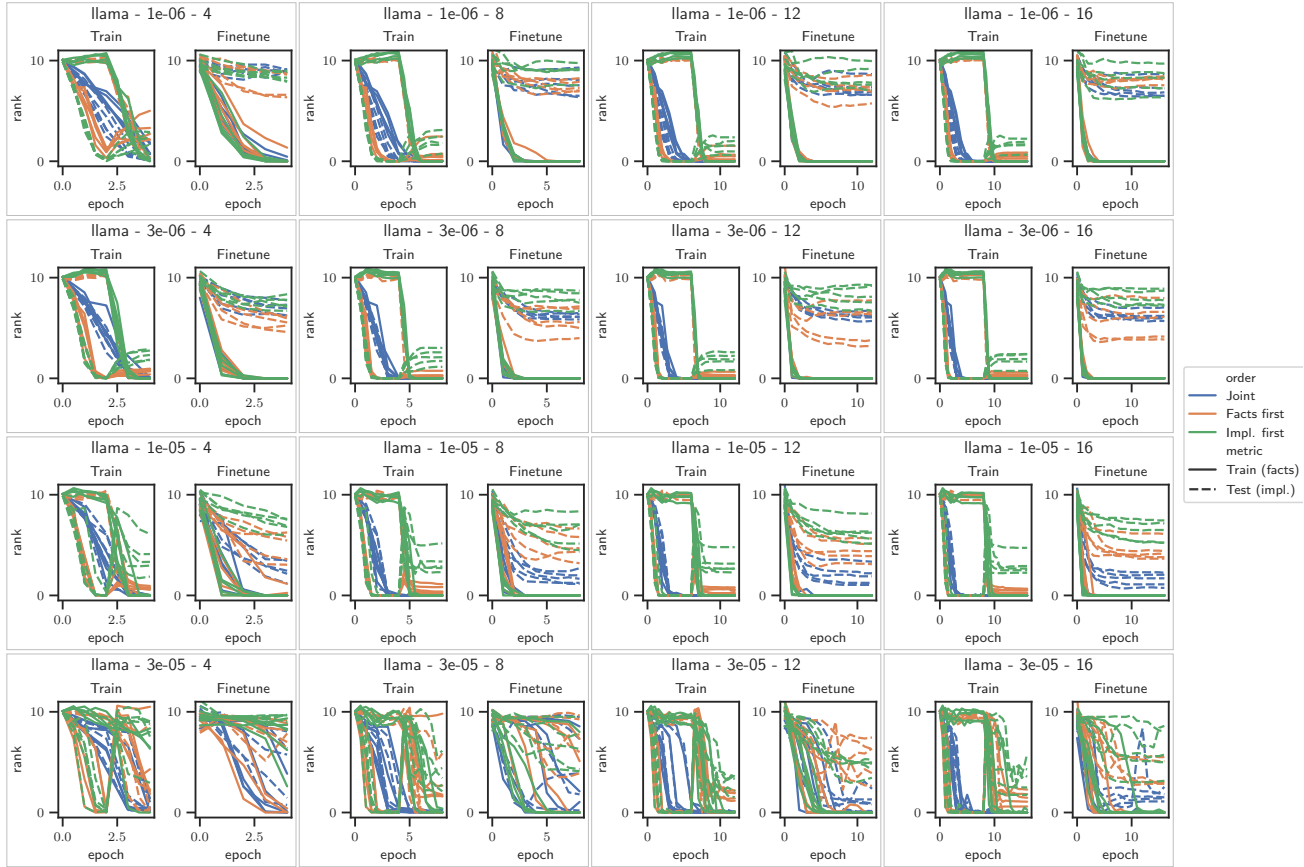


Figure 15. Data ordering effect across different learning rates and epochs for Llama-3-8b. 5 random seeds were used. The title has the format “model - lr - epochs”

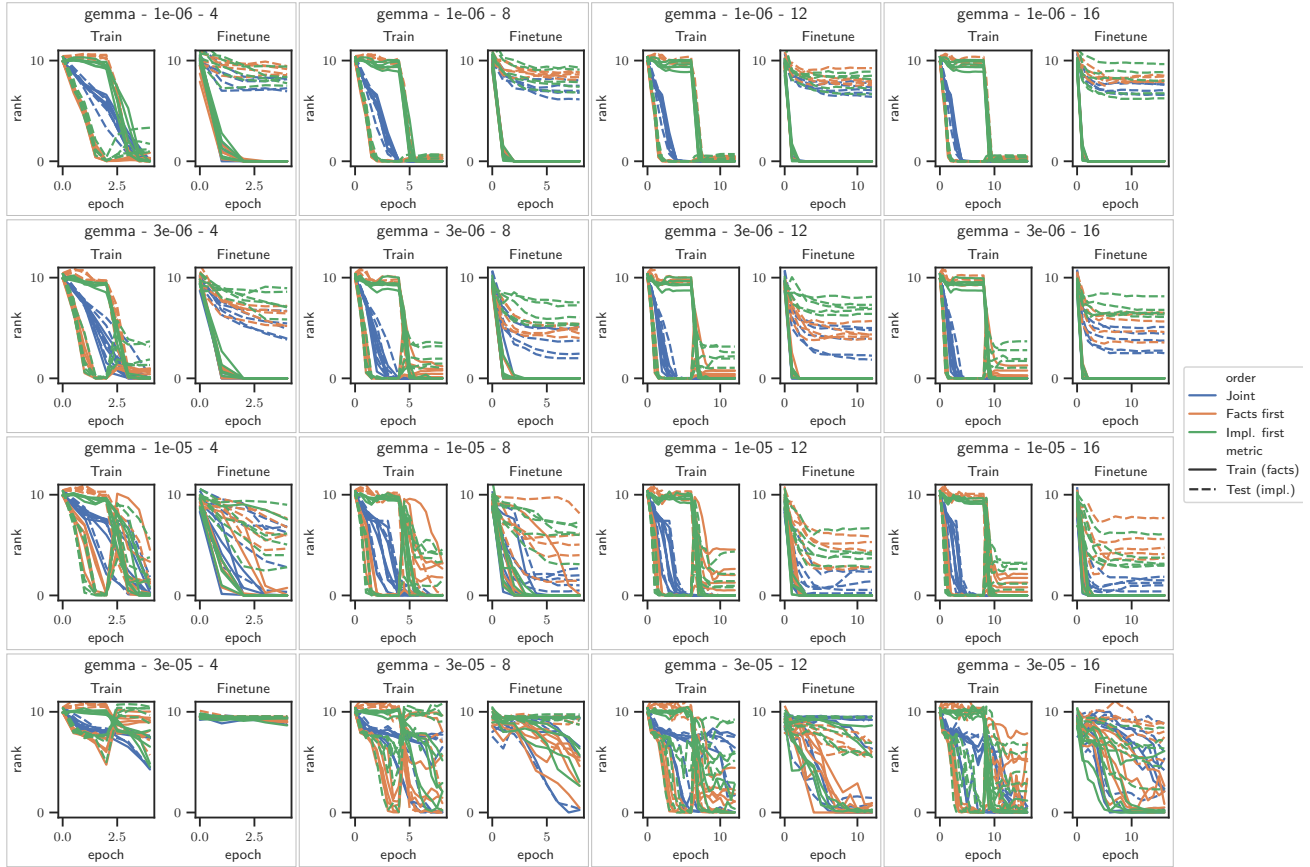


Figure 16. Data ordering effect across different learning rates and epochs for Gemma-2-9B. 5 random seeds were used. The title has the format “model - lr - epochs”

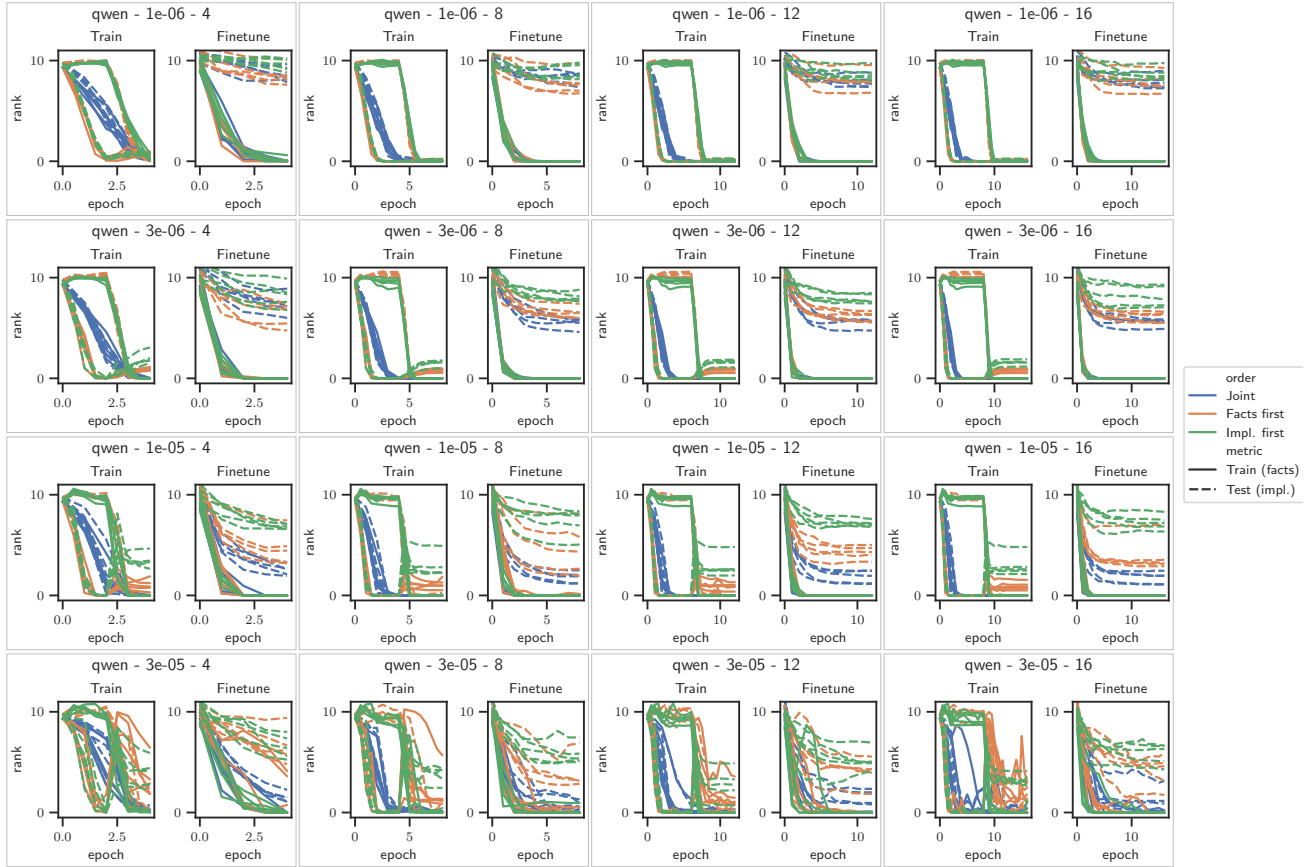


Figure 17. Data ordering effect across different learning rates and epochs for Qwen-2-7B. 5 random seeds were used. The title has the format “model - lr - epochs”

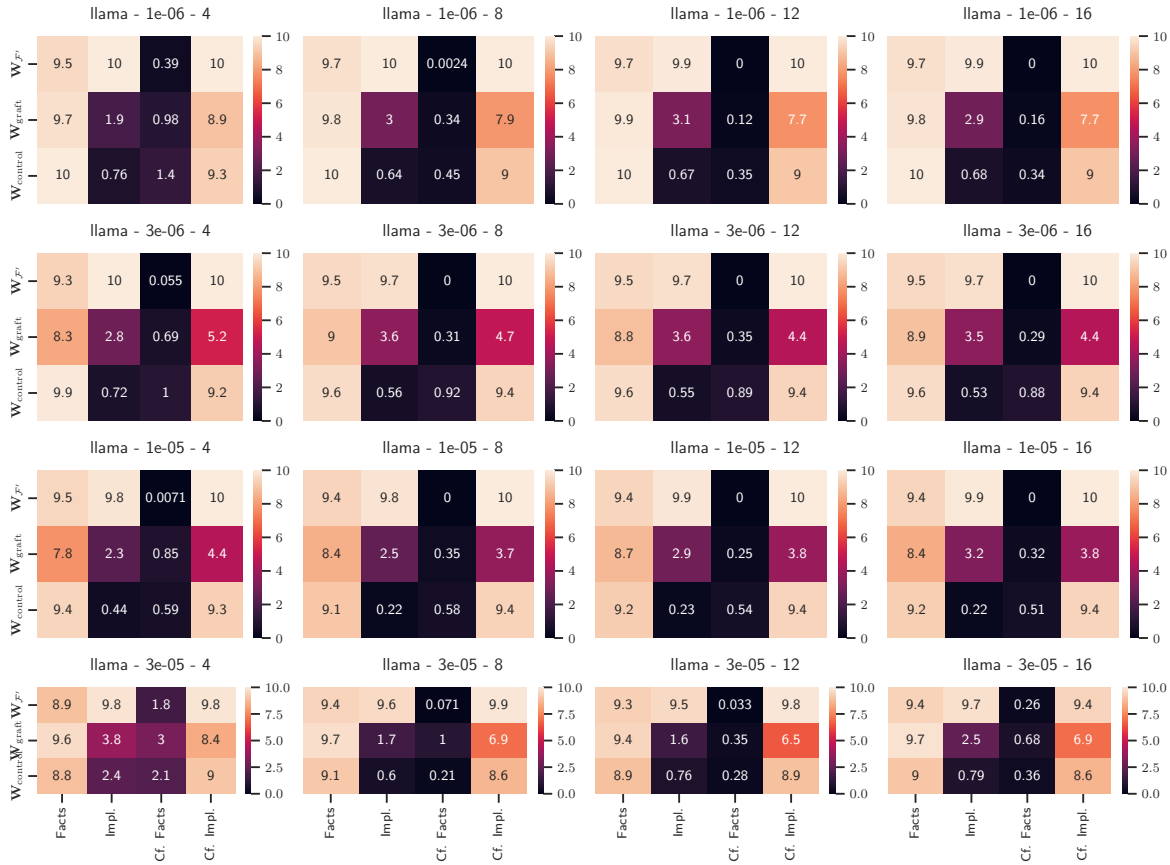


Figure 18. Weight grafting effect across different learning rates and epochs for Llama-3-8b. 5 random seeds were used. The title has the format “model - lr - epochs”

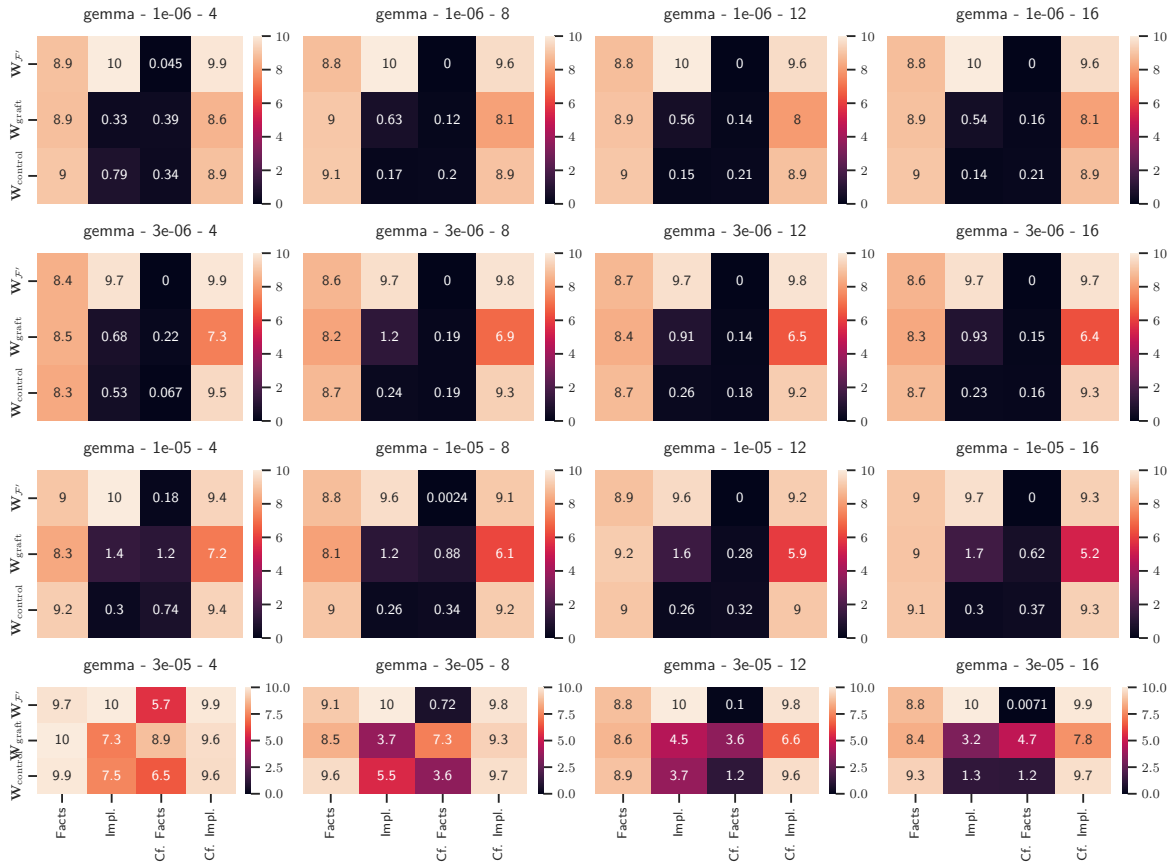


Figure 19. Weight grafting effect across different learning rates and epochs for Gemma-2-9B. 5 random seeds were used. The title has the format “model - lr - epochs”

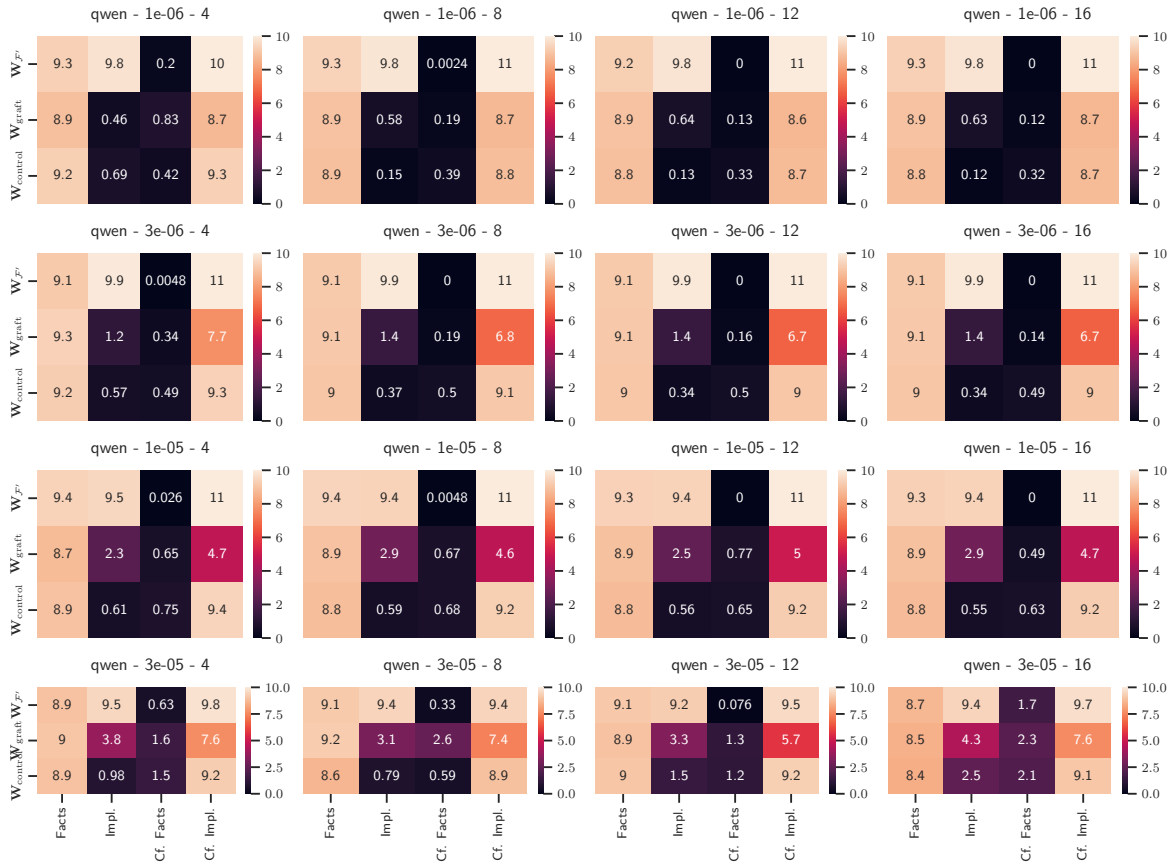


Figure 20. Weight grafting effect across different learning rates and epochs for Qwen-2-7B. 5 random seeds were used. The title has the format “model - lr - epochs”